Performance of a Combined Cyclone-Filter Aerosol Collector

Mason Sangkhamanee

A Thesis Submitted in Partial Fulfillment of the Requirements

for the Degree of Master of Science in Physical Chemistry

Prince of Songkla University

2009

Thesis Title	Performance of a Combined Cyclone-Filter Aerosol Collector
Author	Mr. Mason Sangkhamanee
Major Program	Physical Chemistry

Major Advisor:

…….....
(Asst. Prof. Dr. Surajit Tekasakul)

Co-Advisor:

…….....
(Assoc. Prof. Dr. Perapong Tekasakul)

Examining Committee :

……...……...……...Chairperson
(Assoc. Prof. Dr. Tawatchai Charinpanitkul)

…….…...
(Asst. Prof. Dr. Surajit Tekasakul)

…….…...
(Assoc. Prof. Dr. Perapong Tekasakul)

…….…...
(Asst. Prof. Dr. Orawan Sirichote)

The Graduate School, Prince of Songkla University, has approved this thesis as partial fulfillment of the requirements for the Master of Science Degree in Physical Chemistry

……...……..…
(Assoc. Prof. Dr. Krerkchai Thongnoo)
Dean of Graduate School

...

ชื่อวิทยานิพนธ์	สมรรถนะการดักจับอนุภาคแอโรซอลของอุปกรณ์ที่ประกอบด้วยไซโคลนและแผ่นกรอง
ผู้เขียน	นายเมสันต์ สังขมณี
สาขาวิชา	เคมีเชิงฟิสิกส์
ปีการศึกษา	2552

บทคัดย่อ

ไซโคลนเป็นเครื่องมือชนิดหนึ่งที่ได้รับความนิยมใช้กันอย่างแพร่หลายในวงการอุตสาหกรรม สำหรับดักจับฝุ่นขนาดใหญ่ที่แขวนลอยอยู่ในอากาศก่อนที่จะใช้วิธีอื่นๆ เช่นการกรอง แต่เนื่องจากไซโคลนมีประสิทธิภาพต่ำในการดักจับอนุภาคขนาดเล็ก งานวิจัยนี้จึงได้ทำการดัดแปลงไซโคลนเพื่อให้ประสิทธิภาพในการดักจับอนุภาคขนาดเล็ก (0.3 – 1.0 ไมครอน) สูงขึ้น โดยทำการศึกษาสมรรถนะในการดักจับอนุภาคของอุปกรณ์ที่ประกอบแผ่นกรองเข้ากับไซโคลนแล้วเปรียบเทียบกับไซโคลนเพียงอย่างเดียว ตัวแปรที่ศึกษาได้แก่ ขนาดอนุภาค ความเร็วทางเข้าและคุณลักษณะของแผ่นกรอง ซึ่งตัวแปรเหล่านี้มีผลต่อประสิทธิภาพการดักจับอนุภาคและความดันสูญเสียของไซโคลน จากผลการทดลองพบว่าค่าการทะลุผ่านของไซโคลนมีค่าลดลงเมื่อความเร็วหรือขนาดอนุภาคเพิ่มขึ้น และค่าการทะลุผ่านของไซโคลนสำหรับความเร็วทางเข้าในช่วง 1.84 – 16.72 m s^{-1} มีค่าสอดคล้องกับค่าที่คำนวณได้จากทฤษฎีที่เสนอโดยครอว์ฟอร์ด (Crawford) สำหรับไซโคลนเพียงอย่างเดียวและไซโคลนที่ประกอบกับแผ่นกรองจะให้ประสิทธิภาพการกรองที่ดีกว่า และความดันสูญเสียน้อยลง นอกจากนี้กรณีแผ่นกรองเส้นใยเมื่อความกว้างของแผ่นกรองเพิ่มจาก 4 มิลลิเมตร เป็น 8 มิลลิเมตร พบว่าในช่วงความเร็วทางเข้าที่ศึกษาคือ 1.84 – 16.72 m s^{-1} ค่าการทะลุผ่านที่ลดลงเมื่อเทียบกับไซโคลนจะเพิ่มจาก 0.4 – 2.2% , 0.6 – 6.2% และ 3.2 – 9.4% เป็น 0.3 – 5.5% , 1.3 – 15.8% และ 1.7 – 19.9% สำหรับอนุภาคขนาด 0.3 , 0.5 และ 1.0 ไมครอน ตามลำดับ และค่าความดันสูญเสียที่ลดลงจะเพิ่มจาก 32.7 เป็น 38.8% ส่วนกรณีแผ่นกรองสแตนเลสสตีล เมื่อปริมาณแผ่นกรองเพิ่มขึ้นจาก 0.94 กรัม เป็น 1.83 กรัม ค่าการทะลุผ่านที่ลดลงเมื่อเทียบกับไซโคลนในช่วงความเร็วทางเข้าเดียวกันจะเพิ่มจาก 0.6 – 4.7% , 0.8 – 13.7% และ 1.1 – 20.9 % เป็น 3.7 – 14.8% , 4.3 – 31.2% และ 11.6 – 41.2 % สำหรับอนุภาคขนาด 0.3 , 0.5 และ 1.0 ไมครอน ตามลำดับ และค่าความดันสูญเสียลดลง 23.5 1และ 20.5% ตามลำดับ

Thesis Title Performance of a Combined Cyclone-Filter Aerosol Collector

Author Mr. Mason Sangkhamanee

Major Program Physical Chemistry

Academic Year 2009

ABSTRACT

Cyclone collector is one of the most widely used as industrial devices for coarse particle removal from gas stream, mostly used as the pre-cleaner before other methods such as filtration. This is due to the low collection efficiency of cyclone for fine particles. In this work a lab-scale cyclone was modified by adding filter in the space between the inner core and the wall of the cyclone in order to meet the higher collection performance for the fine particles (0.3 - 1.0 μm). The collection performance of the combined cyclone-filter collector was compared with those of cyclone and filter only. The effects of parameters, such as particle size and inlet velocity, on the collection efficiency and pressure drop were studied. Besides, filter characteristics were also investigated. The results show that the aerosol penetration for the test cyclone collector decreases with increasing inlet velocities or particle sizes. Moreover, the theoretical calculations show the best fit for Crawford model at all inlet velocities. In comparison with the cyclone, the penetration of the cyclone combined with fibrous filter for particle sizes of 0.3, 0.5 and 1.0 μm is found to be lower by 0.4 – 2.2%, 0.6 – 6.2% and 3.2 – 9.4%, respectively, for 4-mm filter width and 0.3 – 5.5% , 1.3 – 15.8% and 1.7 – 19.9%, respectively, for 8-mm filter width. The penetration of the cyclone combined with stainless steel filter is also found to be lower by 0.6 – 4.7% , 0.8 – 13.7% and 1.1 – 20.9%, respectively, for 0.94 g of stainless steel filter and 3.7 – 14.8% , 4.3 – 31.2% and 11.6 – 41.2%, respectively, for 1.83 g of stainless steel filter. Moreover, the pressure drop of the cyclone combined with 4-mm and 8-mm fibrous filter is lower than that of the cyclone by 32.7 and 38.8% for 4 mm and 8 mm fibrous filter, respectively, and 23.5 and 20.5% for 0.94 g and 1.83 g of stainless steel filter, respectively.

ACKNOWLEDGEMENT

I wish to express my deep and sincere gratitude to my advisor, Assistant Professor Dr. Surajit Tekasakul, and Associate Professor Dr. Perapong Tekasakul my co-advisor, for her and his valuable instructions, expert guidance, excellent suggestions and kindness.

My sincere thank is expressed to Assistant Professor Dr. Orawan Sirichote, for her kind help and suggestion.

Special thanks are addressed to Associate Professor Dr. Tawatchai Charinpanitkul for helpful suggestion and effort to thesis examination.

Appreciate thank also goes to the staff of the Department of Chemistry, Faculty of Science, Prince of Songkla University for their support throughout the course of study.

I would like to thank Mr. Prapas Chaitape for his suggestions and help in construction of experimental devices.

I am thankful to the Center of Excellence for Innovation in Chemistry (PERCH-CIC), Commission on Higher Education, Ministry of Education and Graduate School, Prince of Songkla University for financial supports.

Finally, none of this would have been possible without love and encouragement of my family for their kind help and assistance during my study.

Mason Sangkhamanee

CONTENTS

CONTENTS (Continued)

LIST OF TABLES

LIST OF FIGURES

LIST OF FIGURES (Continued)

Page

LIST OF ABBREVIATIONS

a	=	inlet height
b	=	inlet width
d_p	=	particle diameter
d_f	=	fiber diameter
dr	=	thickness of the capture zone
h	=	cylinder height of cyclone
k	=	Boltzmann constant
m_p	=	mass of the particle
n	=	exponent value
r	=	radius of the velocity path
r_1	=	radius of exit outlet
r_2	=	radius of cyclone body
v_r	=	radial velocity
v_θ	=	tangential velocity
A_p	=	particle cross section area
B	=	dust outlet diameter
C_θ	=	Cunningham correction factor
C_d	=	drag coefficient
C_{inlet}	=	concentrations of particles at upstream
C_{outlet}	=	concentrations of particles at downstream
D	=	particle diffusion coefficient
D_c	=	cyclone body diameter
D_e	=	gas exit diameter
E	=	efficiency
F_c	=	centrifugal force

LIST OF ABBREVIATIONS (Continued)

F_d	=	drag force
H	=	cyclone height
L_c	=	cone length of cyclone
N_{in}	=	number concentration of particles at the upstream
N_{out}	=	number concentration of particles at the downstream
P	=	penetration
Q	=	flow rate
R	=	interception parameter
R_f	=	fiber radius
S	=	vortex finder length
T	=	absolute temperature
U	=	inlet velocity
U_0	=	face velocity of filter
V	=	volumetric flow rate
V_0	=	inlet volumetric flow rate
V_r	=	particle radial velocity
V_{r_2}	=	particle radial velocity at outer radius of cyclone
V_s	=	secondary volumetric flow rate
V_{TS}	=	terminal settling velocity
V_θ	=	particle tangential velocity
V_{θ_2}	=	particle tangential velocity at outer radius of cyclone
S	=	vortex finder length
Z	=	filter thickness
λ	=	mean free path of the gas molecules
α	=	pressure drop coefficient
α_f	=	packing density of filter

LIST OF ABBREVIATIONS (Continued)

μ_g	=	viscosity of air
ρ_g	=	density of gas
ρ_p	=	density of particle
ω	=	angular velocity
θ	=	traveling angle of particle
θ_1	=	turning angle of particle
ϕ	=	filtration area
Δp	=	pressure drop across the cyclone
Δp_0	=	pressure drop across the fibrous filter
τ	=	relaxation time
η	=	single-fiber efficiency
η_{inter}	=	single-fiber efficiency by interception
η_{imp}	=	single-fiber efficiency inertial impaction
η_{diff}	=	single-fiber efficiency by diffusion

CHAPTER 1
INTRODUCTION

1.1 General Background

Cyclones, the particulate collectors using centrifugal force to separate the particles from dust-laden gas flows, are widely used in the field of industrial particulate control because of the simple structure and low-cost in operation. Moreover, they can withstand high temperatures and pressures. Cyclone collector is mostly used for the collection of medium-sized and coarse particles. They can be used effectively for particulates generally larger than 10 μm (Jiao et al, 2006). However, the collection efficiency is low for fine particles. They are generally used as upstream precleaners of other devices to reduce the dust loading and to remove larger, abrasive particles.

There are two methods to improve cyclone performance: one is to optimize the configurations and geometric dimensions of the cyclones and the other is to equip additional separation devices to the cyclones. Stairmand high-efficiency cyclone is the result of the first method (Stairmand, 1951), adjusting the cyclone configuration to meet the high-efficiency and acceptable pressure drop requirement of the lab-scale cyclone. However, optimized cyclone still cannot meet the requirements of fine particle separation. Thus, some researchers have seeked an alternative approach by introducing additional devices to obtain higher separation efficiency, for example: the double cyclone (Lim et al, 2004a), an additional cylinder exists between the outer wall and the gas outlet compared to the conventional cyclone; double inlet cyclone (Lim et al, 2003), a cyclone with a inlet divided into two.

1.2 Literature Review

In order to understand how to improve the cyclone performance for the fine particles, modification of cyclone configuration and addition of separation

devices are studied. In the past, improvement of the cyclone for fine particles has been investigated by many researchers. It will be reviewed here.

1.2.1 Configuration of Cyclones

Lim et al. (2004a) studied the collection efficiency of the conventional cyclone with different vortex finder diameters (7 and 23 mm), and vortex finder lengths (23, 46 and 69 mm) and compared the results with the double cyclone. It was found that the smaller vortex finder diameter (7-mm), the higher collection efficiency because a well-defined outer spiral flow and a small and long inner spiral flow is formed. The cyclone with shortest vortex finder length (23-mm) shows the highest collection efficiency. Since the longer vortex finder causes the flow field inside cyclone becomes turbulent. The collection efficiency of the double cyclone is higher than that of the conventional cyclone with 23-mm vortex finder diameter, but lower than that with 7-mm vortex finder diameter. An additional vortex might not form in the annular spaces or the intensity of the vortex may not be strong enough to separate particles in the double cyclone.

Lee et al. (2006) investigated the effects of the cylinder shape on the flow characteristics and particle collection efficiency. The cyclone with a conical section twice as long as that of the Stairmand cyclone was used. It was found that the long-cone cyclone has unstable flow field near the bottom of the view finder or air outlet duct, unlike the Stairmand cyclone. The flow field is not fully developed and stable in the cylinder region due to the sharp transition to conical section. This resulted in the short circuiting flow at the view finder opening and adversely affected the particle collection efficiency. The short-circuiting completely disappears when the cylinder diameter is increased by 20%. It was also confirmed that the axial velocity profiles show an M-shape throughout the entire improved long-cone cyclone region, as in the case of the well-designed Stairmand cyclone. The overall collection efficiency of the improved cyclone increases about 2-3%, with no increase in pressure loss.

Chen et al. (2006) studied the effect of the vent-pipe insert depth and the modified edge-sloped vent-pipe shape on the collection efficiency and pressure drop. The results showed that the collection efficiency rises with the increase of vent-pipe insert depth, which reduces the probability of short-circuiting flow. However, when the vent-pipe is inserted extremely deep, the flow field inside becomes turbulent which may lead to more exit of the coarser particles at the top with the carrier gas by re-entrainment. For the modified edge-sloped vent-pipe cyclone, both collection efficiency and pressure drop drawns the orientation of the sloped edge: the maximum at 90° and the minimum at 270°. Under the same condition, the pressure drop of the modified cyclone is about 10% higher than that of the conventional cyclone.

1.2.2 Additional Devices

Wu et al. (2000) investigated the collection performance of oil droplets by a cyclone with unwoven fabrics attached to inner wall of the outlet tube. Oil droplets of lubricant were generated either by an oil mist lubrication unit or a two-fluid nozzle. The first generator was used to generate relatively small droplet at high concentration: mass median aerodynamic diameter (MMAD) was 2.2 μm, geometric standard deviation (GSD) was 1.95 μm and mass concentration was 0.97 g m^{-3}. The second generator was for relatively large oil mist with a high mass concentration: MMAD was 5.8 μm, GSD was 2.15 μm and mass concentration was 200 g m^{-3}. The overall collection efficiency of an unmodified cyclone was 43%, the 50% cut-off size was 3.1 μm and the pressure drop was 550 Pa. Furthermore, it was noticed that the collection efficiency of droplet larger than about 7 μm decreased because of the re-entrainment of large droplets from the oil film. When the polypropylene fabric with thickness of 1 mm was attached, the overall collection efficiency was increased to 50.9% and the 50% cut-off size was decreased to 2.86 μm. However, the polyester fabric with thickness of 2.5 mm significantly increased the overall collection efficiency to 76.9% and reduced the 50% cut-off size to 1.5 μm. Furthermore, no decrease in the collection efficiency for droplets larger than 5 μm due to the re-

entrainment from the oil film was observed. The pressure drop of cyclone with the polyester fabric was increased to 750 Pa.

Jo et al. (2000) investigated the collection efficiency for the fine particles of a reverse flow cyclone in combination with a post cyclone (PoC) to the gas exit duct. The PoC consists of two cylindrical shells, arranged in an annular configuration and placed on the exit duct of a reverse flow cyclone. When the test velocity is in the range of 4.9-23.2 m s^{-1}. The results showed that the overall efficiency of the cyclone combined with the PoC is higher than that of the cyclone alone for 2-20% depending of on the operating conditions and the size of the cyclone. The pressure drop over the PoC is approximately 10% of the total pressure drop over the cyclone. Although the PoC is quite effective for the removal particles between 3 and 10 μm, a collection of particles below 3 μm cannot be improved significantly.

Wang et al. (2005) studied the insertion of a stick into the cyclone. One end of the stick is fixed at the point (radius of 54 mm and direction of 175°) on the top cover of the cyclone separator, and the other is fixed at the cone bottom in the same azimuth. The turbulence structures of the flow field were observed using Laser Doppler Velocimetry (LDV). The results showed that the insertion of a stick decreased the mean tangential velocity remarkably and increases the turbulence intensity. Besides the insertion of a stick also change the original vortex flow field to be non-axisymmetrical, and reduce the pressure drop of cyclone collector. This is due to the stick reduces the rotational kinetic energy more than increases the turbulent energy.

1.2.3 Basic Parameters

Fassani and Goldstein Jr. (2000) studied the effect of high inlet solid loadings on cyclone pressure drop and collection efficiency using a fluid catalytic cracking (FCC) catalyst with a single size distribution and Sauter mean diameter of 35.95 μm. The range of concentrations was extended up to 20 kg of solids/kg of gas

and the average entrance velocities were 7, 18 and 27 m s^{-1}. It was observed that the higher the velocity, the higher the pressure drops, independent of solid loading. The results also showed that the present of particles in the gas stream reduced the cyclone pressure drop, compared to the dust free flow. The dust laden air flow pressure drop may be estimated as 47% of the clean air flow pressure drop. The phenomenon is due to a reduction of the tangential gas velocity, caused by an increase in wall friction or the equalization of the gas momentum of adjacent layers by particle inertia. The collection efficiency increases with concentration until up to 12 kg of solids/kg of gas, then it has a tendency of reduction.

1.3 Research Objectives

In the present work, an attempt has been made to improve the collection performance of cyclone for the fine particles, smaller than 1 μm, by using combination of filter and cyclone. The objectives of this work are:

1. To investigate the fine particle collection performance of a combined cyclone-filter collector in comparison with a regular cyclone by varying basic operating parameters which are inlet velocity, particle size, filter configuration, and filter characteristic.
2. To compare the theoretical values of cyclone performance with experimental data.

CHAPTER 2
THEORY

2.1 Cyclone Collectors

Cyclone collector is a gas cleaning device that employs a centrifugal force generated by a spinning gas stream to separate the particulate matter (solid or liquid) from the carrier gas. It is probably the most widely used equipment in any industrial and other purposes. The typical cyclone collectors are usually employed for removing particles larger than 10 μm. However, conventional cyclones seldom remove particles with an efficiency greater than 90 percent unless the particle is 25 μm or larger. In practice, it has been worked out to place a large number of small cyclones in parallel in order to treat a large amount of polluted air or in series when the higher efficiency is required.

2.2 Principles of Cyclone Collectors

In principle, the polluted air entering the tangential inlet on the top of cylindrical body of cyclone creates descending vortex as shown in Fig. 2.1. The flow moves in spiral pattern downward between the walls of the clean air outlet and the inner wall of the cyclone. When the air comes near the bottom of the cone, the vortex reverses its direction of axial flow but maintains its direction of rotation which is called ascending vortex; traveling upward to the air outlet or vortex finder. Dust particles are centrifuged toward the wall and collected by inertial impingement. The collected dust flows down in the gas boundary layer to the cone apex where it is discharged through a dust hopper. Thus there are four basic steps involved in cyclone operation: dust concentration, descending vortex, dust discharge and ascending vortex.

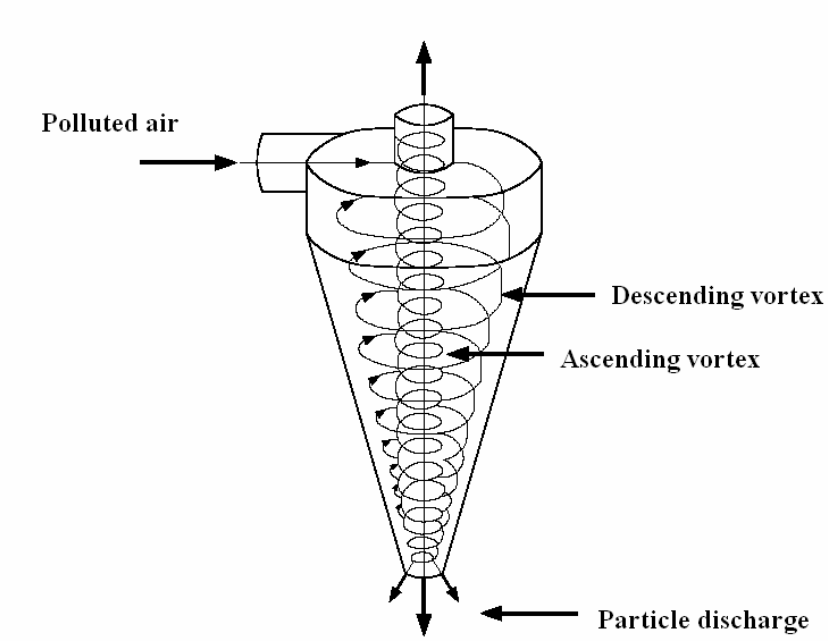

Figure 2.1 Basic cyclone configuration showing flow direction.

Dust Concentration

The polluted air entering the top parts of cyclone. Under centrifugal force, dust particles move toward to the cyclone wall because of its inertial force. Dust particles are concentrated near the walls.

Descending Vortex

Dust particles of large diameter which are separated along the wall are carried down by the helical stream of gas in the cyclone body and cone. These dust particles are ultimately discharged in the dust bin. The gas reverses its direction and enters the ascending vortex.

Dust Discharge

The dust consists of particles which are concentrated near the wall and away from the ascending vortex. They are then carried out downwards. The dust is discharged at the apex of the cone. The ascending vortex actually starts somewhere in the hopper of dust bin below the cyclone cone. The dust particulates with some gas must be carried into the hopper. If too much gas is carried into the hopper, collected dust may be re-entrained and carried up by the ascending vortex.

Ascending Vortex

The gas from the descending vortex reverses its direction and goes up from the bottom to the top. The length of the ascending vortex is from the dust outlet to the outlet of the gas exhaust duct.

2.3 Types of Cyclone Collectors

Cyclones can be divided into three classes in the point of view of their efficiency (Storch et al., 1979): high efficiency cyclone (98-99% efficiency), conventional cyclone (70-80% efficiency), and high throughput cyclone (50% efficiency) as displayed in Fig. 2.2. Among these three cyclone types, high efficiency cyclone is likely to have the highest pressure drop and smallest body diameter, while high throughput cyclone can treat large volume of gas with a low pressure drop.

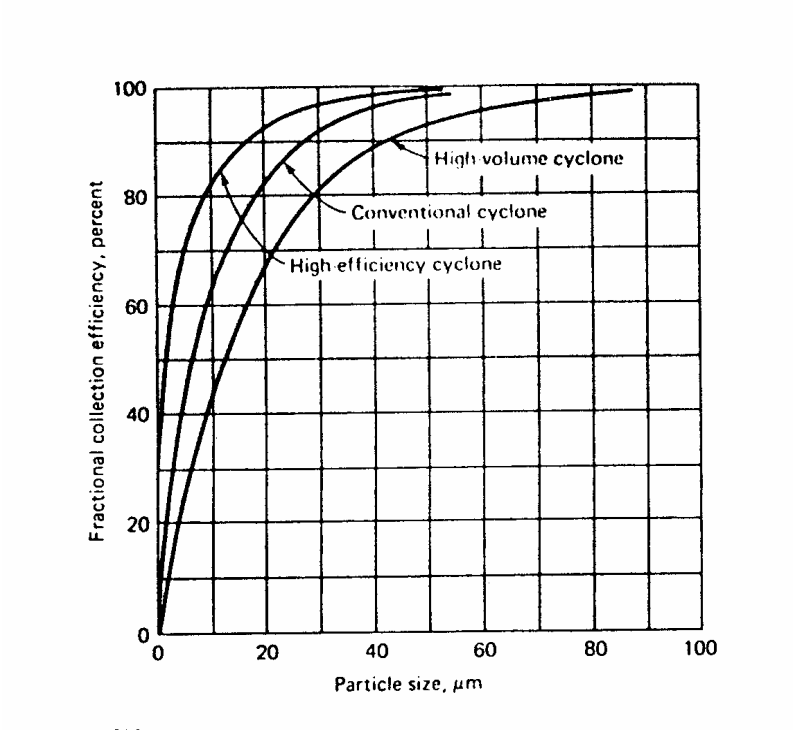

Figure 2.2 Fractional collection efficiency as a function of particle size for several types of cyclone (Stern et al., 1968).

Each type of these three cyclones has the same basic configuration. Different levels of collection efficiency are achieved by varying the standard cyclone dimensions, identified in Fig 2.3, according to the values shown in Table 2.1 (Wolfgang ang Vincent, 1980).

Table 2.1 Dimensions of standard cyclone (Wolfgang ang Vincent, 1980)

Cyclone dimension	High Efficiency		Conventional			High Throughput	
	Stairmand (1951)	Swift (1969)	Lapple (1967)	Swift (1969)	Peterson &Whitby (1965)	de Nevers (1995)	Heinsohn & Kabel (1999)
Body diameter, D_c/D_c	1.0	1.0	1.0	1.0	1.0	1.0	1.0
Inlet Height, a/D_c	0.5	0.44	0.5	0.5	0.583	0.75	0.8
Inlet Width, b/D_c	0.2	0.21	0.25	0.25	0.208	0.375	0.35
Gas Exit Diameter, D_e/D_c	0.5	0.4	0.5	0.5	0.5	0.75	0.75
Vortex Finder Length, S/D_c	0.5	0.5	0.625	0.6	0.583	0.875	0.85
Cylinder height, h/D_c	1.5	1.4	2.0	1.75	1.333	1.5	1.7
Cone Length, L_c/D_c	2.5	2.5	2.0	2	1.837	2.5	2.0
Dust Outlet Diameter, B/D_c	0.375	0.4	0.25	0.4	0.5	0.375	0.4

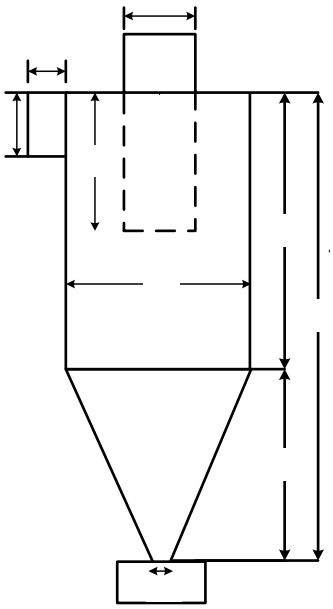

Figure 2.3 Schematic diagram of standard cyclone.

One cyclone may be classified in more than one class, depending upon the particle size being collected, as shown in Table 2.2 (Stern and Knowlton, 1968).

Table 2.2 Overall cyclone collection efficiency (Stern and Knowlton, 1968).

Particle size range (μm)	Conventional cyclone	High-efficiency
< 5	<50	50-80
15-20	50-80	80-95
15-40	80-95	95-99
>40	95-99	95-99

2.4 Particle Collecting Mechanisms

The separation mechanism of cyclone separators is based on a vortex motion, causing the centrifugal force to separate particles from the cleaned air, the particles move away from the cyclone axis towards cyclone wall.

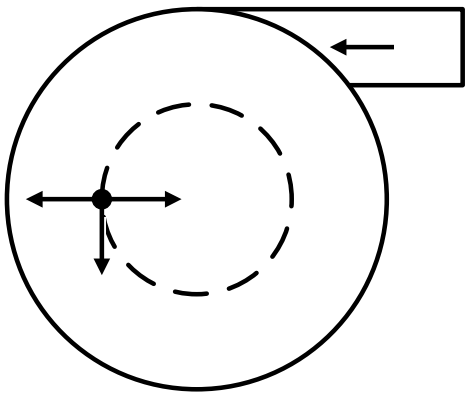

Figure 2.4 The forces acting on a particle in a fluid.

There are many forces acting on a particle in cyclone collector, including centrifugal force, drag force and gravity force. However, the movement in the radial direction is the result of two opposing forces where the centrifugal force acts to move the particle to the wall, while the drag force of the air acts to carry the particles into the axis. As the centrifugal force is predominant, separation takes place. Fig. 2.4 shows the forces acting on a spherical particle settling through a fluid under the influence of centrifugal force and drag force. Writing Newton's law for the particle, we obtain

$$F_c - F_d = m\frac{dv}{dt} \tag{2-1}$$

$$\frac{\pi d_p^3}{6}\rho_p \omega^2 r - C_d A_p \rho_p \frac{v_r^2}{2} = m_p \frac{dv_r}{dt} \tag{2-2}$$

where d_p is the particle diameter (m), ρ_p is the particle density (kg m^{-3}), ω is the angular velocity (rad s^{-1}), r is the radius of the velocity path (m), C_d is the drag coefficient, A_p is the particle cross section area (m^2), v_r is the radial velocity of the particle (m s^{-1}) and m_p is the mass of the particle (kg).

The first left-side term (F_c) is the centrifugal force on each particle which occurs when it travels around the cyclone axis. Its magnitude depends mainly on three factors: mass of each particle, radius of spiral motion and particle velocity. The second left-side term (F_d) is the drag force which is the force that resists the movement of a solid object through a fluid. The drag is the sum of all the aerodynamic forces in the direction of the external fluid flow.

2.5 Cyclone Collection Efficiency

The most important parameters of a cyclone performance are its collection efficiency and the pressure drop across the unit. The meaning of cyclone efficiency is defined as its ability to capture and retain dust particles whereas the

pressure drop is the amount of power that the unit need to process. In collection of particle, the penetration of particles is usually used rather than the collection efficiency in order to understand the penetration characteristics of the collectors. Penetration (P) of the collector is defined as:

$$P = 1 - E \tag{2-3}$$

where E is the collection efficiency. In this work, the penetration will be used.

2.5.1 Collection Efficiency Models

In order to verify the experimental setup, three theoretical models: Crawford, Mixed flow and Leith & Licht model will be used to calculate the penetration of the test cyclone.

2.5.1.1 Crawford's Model (Crawford, 1976)

In Crawford's model for a reverse-flow cyclone collector, the effect of laminar layer next to the outer edge of the cyclone is considered, as shown in Fig. 2.5 such that all particles which enter it are captured. This model is based on the following assumptions.

- Neglecting boundary-layer effects, therefore no secondary flows induced by the presence of sidewalls (no friction exists in the flow).
- The particle is moving at its terminal velocity at all points along its trajectory.
- The effect of the turbulent eddies is to distribute the particles uniformly over the cross section at any given angle θ

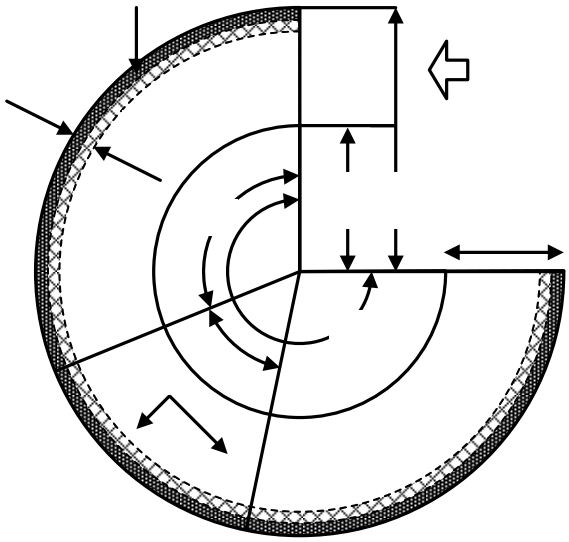

Figure 2.5 Turbulent cyclone flow.

The penetration of dust for the reverse-flow cyclone was suggested to be calculated from the following expression:

$$P = \exp\left(-\frac{\rho_p Q \; d_p^2 \theta_1}{36\mu_g a(r_2 - \sqrt{r_1 r_2})(r_2 - r_1)} \right) \qquad (2\text{-}4)$$

where the total turning angle θ_1 becomes

$$\theta_1 = \frac{2\pi(h + L_c/2)}{a} \qquad (2\text{-}5)$$

where Q is the flow rate ($m^3\ s^{-1}$), θ_1 is the total turning angle (rad s^{-1}), μ_g is the gas viscosity (kg $m^{-1}\ s^{-1}$), a is the inlet height of cyclone (m), r_1 is the radius of exit duct, r_2 is the radius of cyclone body, h is cylindrical height of cyclone (m), and L_c is cone height of cyclone.

2.5.1.2 Leith and Licht Model (Leith and Licht, 1972)

Leith and Licht described particle motion in the entry and collection regions with the additional following assumptions:

- The tangential velocity of a particle is equal to the tangential velocity of the gas flow, that is, there is no slip in the tangential direction between the particle and the gas.
- The tangential velocity is related to the radius by: uR^n = constant.

The particles penetration could be described by the following expression:

$$P = \exp\left(-2\left(\frac{G\tau V_0}{D_c^3}(n+1) \right)^{0.5/n+1} \right) \tag{2-6}$$

where G is a factor related to the configuration of the cyclone (-), τ is the relaxation time (s), V_0 is the inlet volumetric flow rate ($m^3\ s^{-1}$), D_c is the cyclone body diameter (m), n is the vortex coefficient (-).

The factor describing the geometric configuration becomes

$$G = \frac{4D_c(2V_s + V)}{a^2 b^2} \tag{2-7}$$

where V_s is the secondary volumetric flow rate ($m^3\ s^{-1}$), V is the volumetric flow rate ($m^3\ s^{-1}$).

The secondary volumetric flow rate and the volumetric flow rate are calculated from

$$V_s = [\pi(S - a/2)(D_c^2 - D_e^2)]/4 \tag{2-8}$$

$$V = \frac{\pi D_c^2}{4}(h - S) + (\frac{\pi D_c^2}{4})(\frac{H - h}{3})(1 + \frac{B}{D_c} + \frac{B^2}{D_c^2}) - \frac{\pi D_e^2}{4}(H - S) \tag{2-9}$$

where S is vortex finder length (m), h is the cylinder height of cyclone (m), H is the cyclone height (m), B is the dust outlet diameter (m), D_e is the gas exit diameter (m).

The relaxation time is calculated by

$$\tau = \frac{\rho_p d_p^2}{18\mu} \tag{2-10}$$

The vortex exponent becomes

$$n = 1 - \left(1 - \frac{(12D_c)^{0.14}}{2.5}\right)\left(\frac{T + 460}{530}\right) \tag{2-11}$$

where T is the absolute temperature (K).

2.5.1.3 Mixed Flow Model (de Nevers, 1995)

This model is applied from the gravity settler which the outer helix is equivalent to the gravity settler. This model is based on the following assumptions.

- No mixing in the direction of fluid flow (x, horizontal)
- The gas flow is totally mixed in transverse direction (y, horizontal, or z vertical)

The penetration for the mixed flow could be described as the following:

$$P = \exp - \left(\frac{\pi N_t V_c d_p^2 \rho_p}{9 b \mu_g} \right) \tag{2-12}$$

where N_t is the number of turns that the gas makes traversing the outer helix, V_c is circular velocity (m s^{-1}), b is the inlet width (m).

The number of turns is calculated by

$$N_t = \frac{1}{a} \left(h + \frac{L_c}{2} \right) \tag{2-13}$$

2.5.2 Collection Efficiency Parameters

Cyclone efficiency has been widely studied and generally shown to increase with the following parameters: increasing cyclone length that provides a longer residence time of gas (Stern and Knowlton, 1968); reducing vortex finder diameter and increasing vortex finder length which cause a well-defined outer spiral flow (Kim and Lee, 1990), modifying the bottom of vortex finder to be cone-shape which reduces the re-entrainment of separated particles (Lim et al., 2004b).

Conversely, efficiency of cyclone will decrease with increasing in following parameters: cyclone wall roughness which causes local eddy currents and reduces vortex intensity, gas viscosity or density, cyclone diameter, gas outlet diameter, and inlet duct area. Another common cause of cyclone ineffectiveness is leakage of air into the dust outlet. Especially, this will decrease the efficiency for fine particles.

2.6 Pressure Drop Across Cyclone

Pressure drop across a cyclone is an important parameter in the evaluation of cyclone performance. It is the work required to operate the cyclone. The cyclone pressure drop is a function of cyclone dimensions and its operating conditions. However, it is well known that the pressure drop is proportional to square of the inlet velocity. The empirical model used for the prediction of pressure drop is (Jolius et al., 2005)

$$\Delta p = \alpha \frac{\rho_g U^2}{2} \tag{2-14}$$

where α is the pressure drop coefficient depending upon the geometrical parameters of cyclone (-), U is inlet velocity (m s^{-1}).

There are four models employed in this work: Shepherd and Lapple model (Shepherd and Lapple, 1939), Casal and Martinez model (Casal and Martinez, 1983), Dirgo model (Dirgo, 1988) and Coker model (Coker, 1993). The pressure drop coefficients of these models are listed in Table 2.3.

Table 2.3 The empirical models of pressure drop coefficient (α).

Model	α
Shepherd and Lapple	$\alpha = 16\frac{ab}{D_e^2}$
Casal and Martinez	$\alpha = 11.3\left(\frac{ab}{D_e^2}\right)^2 + 3.33$
Dirgo	$\alpha = 20\left(\frac{ab}{D_e^2}\right)\left[\frac{S/D_c}{(H/D_c)(h/D_c)(B/D_c)}\right]^{1/3}$
Coker	$\alpha = 9.47\frac{ab}{D_e^2}$

2.7 Filtration Theory

Filtration is a physical operation which is used for the separation of particles from gas streams by interposing a filter to the gas streams. Only gas can pass while the particles are captured. Collection efficiency of the filter depends upon the pore size, packing density, face velocity, particle size and the thickness of the filter as well as the mechanisms that occur during filtration.

2.7.1 Filtration Efficiency

Generally, the collection efficiency (E) of filter is characterized by: the fraction of entering particles retained by the filter. On the other hand, is usually characterized in terms of its penetration (P): the fraction of entering particles that exit or penetrate the filter, its can be expressed in terms of a particle number (N):

$$P = \frac{N_{out}}{N_{in}} = 1 - E \qquad (2\text{-}15)$$

2.7.2 Single-Fiber Efficiency

To characterize fibrous filtration, the capture of particles by a single fiber will be considered. The single-fiber efficiency (η) is defined as the ratio of the number of particles striking the fiber to the number which would strike if the streamlines were not diverted around the fiber (Baron and Willeke, 1994). If a fiber of radius R_f removes all the particles contained in a layer of thickness Y as shown in Fig. 2.6, the single-fiber efficiency is then defined as Y/R_f .

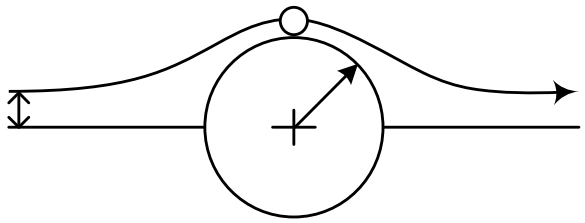

Fig. 2.6 Definition of the single-fiber efficiency.

The overall efficiency (E), of a filter composed of many fibers in a mat can be related to the single fiber efficiency as follows (Baron and Willeke, 1994):

$$E = 1 - \exp\left[\frac{-4\eta\alpha_f Z}{\pi d_f (1-\alpha_f)}\right] \tag{2-16}$$

where η is the single-fiber efficiency, α_f is the solidity or packing density of the filter, Z is the filter depth or thickness, and d_f is the fiber diameter.

Y

2.7.3 Filtration Mechanisms

As air penetrates a filter, the trajectories of particles deviate from the streamlines due to several mechanisms. As a result, particles may collide with the fiber surface and become deposited on them. The important mechanisms causing particle deposition are diffusion, interception, inertial impaction, and gravitational settling.

Diffusion

Under normal conditions, aerosol particles undergo Brownian motion. Small particles generally do not follow the streamlines but continuously diffuse away from them. Once a particle is captured on a surface, it would adhere to it due to the van der Waals force. The trajectory of one such particle is shown in Fig. 2.7 (Hinds, 1999).

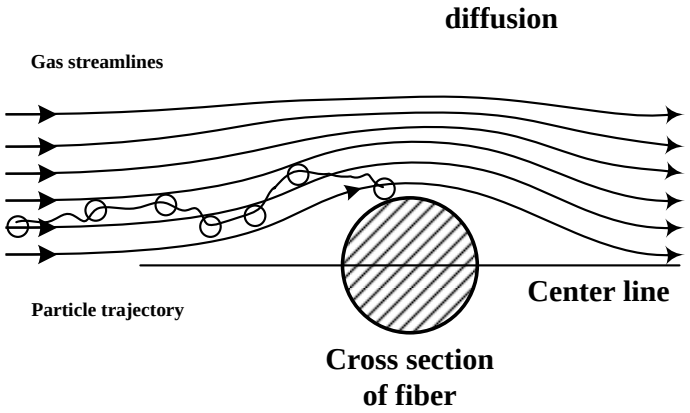

Figure 2.7 Single-fiber collection of a particle by diffusion.

Brownian motion generally increases with decreasing particle size, the diffusive deposition of particles is increased when the particle size is reduced. This phenomenon is illustrated in Fig. 2.8. Similarly at low air velocities, particles can spend more time in the vicinity of the fiber surfaces, thus enhancing diffusional

collection. From the convective diffusion equation describing this process, a dimensionless parameter called the Peclet number (Pe) is defined as

$$Pe = \frac{d_f U_0}{D} \tag{2-17}$$

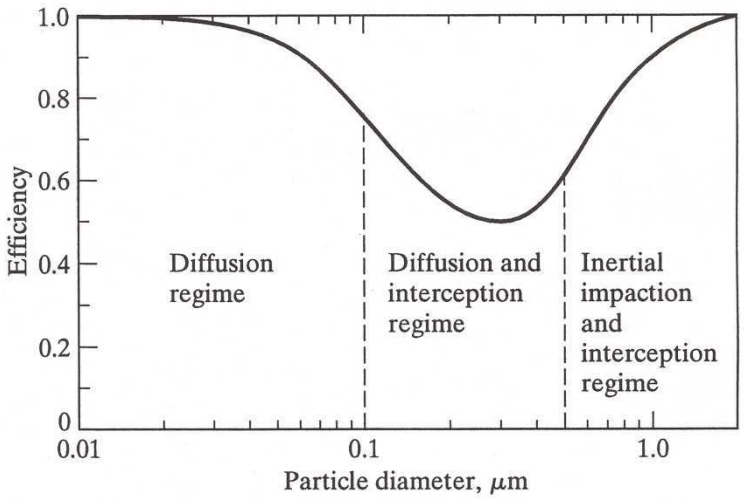

Figure 2.8 Filter collection efficiency versus particle size illustrating the different filtration regimes (Baron and Willeke, 1994).

where d_f is the fiber diameter, U_0 is the face velocity of filter, and D is the particle diffusion coefficient. For pure molecular diffusion (D) is expressed as

$$D = \frac{kTC_c}{3\pi\mu d_p} \tag{2-18}$$

where k is the Boltzmann constant, T is the absolute temperature. From the above discussion, particle collection by diffusion is expected to decrease with increasing Peclet number. The Cunningham correction factor (C_c) can be written as

$$C_c = 1 + 2.492\frac{\lambda}{d_p} + 0.84\frac{\lambda}{d_p}\exp\left(-0.435\frac{d_p}{\lambda}\right)$$

where λ is the mean free path of the gas molecules

The single-fiber efficiency by diffusion (η_{diff}) was developed by Lee and Liu (1982):

$$\eta_{diff} = 2.58\left(\frac{1-\alpha_f}{Ku}\right)^{1/3} Pe^{-2/3} \tag{2-19}$$

where Ku is the Kuwabara hydrodynamic factor, a dimensionless factor that compensates for the effect of distortion of the flow field around the fiber because of its proximity to other fibers, defined as

$$Ku = -\frac{1}{2}\ln\alpha_f - \frac{3}{4} + \alpha_f - \frac{\alpha_f^2}{4} \tag{2-20}$$

Interception

Even if the trajectory of a particle does not depart from the streamline, a particle may still be collected if the streamline brings the particle center to within one particle radius from the fiber surface as shown in Fig. 2.9. One would expect the interception to be relatively independent of flow velocity for a given fiber, and this characteristic can be contrasted to the flow-dependent characteristics of diffusion and inertial impaction. The dimensionless parameter describing the interception effect is the interception parameter (R) defined as the ratio of particle diameter to fiber diameter:

$$R = \frac{d_p}{d_f} \tag{2-21}$$

where d_f is fiber diameter (m).

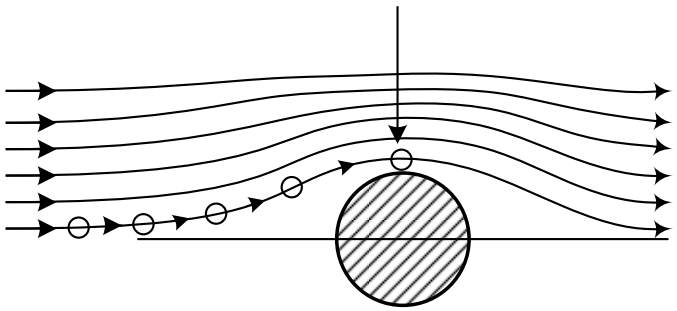

Figure 2.9 Single-fiber collection of a particle by interception.

The single-fiber efficiency by interception (η_{inter}), using the Kuwabara flow can obtain the following expression:

$$\eta_{inter} = \frac{1+R}{2Ku}\left[2\ln(1+R) - 1 + \alpha_f + \left(\frac{1}{1+R}\right)^2\left(1-\frac{\alpha_f}{2}\right) - \frac{\alpha_f}{2}(1+R)^2\right] \quad (2\text{-}22)$$

where η_{inter} is the single-fiber efficiency due to interception. Although Eq. (2-22) is a complete expression for the interception efficiency, the equation is somewhat long, and it can be approximated into the following simpler form:

$$\eta_{inter} = \frac{1-\alpha_f}{Ku}\frac{R^2}{(1+R)} \quad (2\text{-}23)$$

Inertial impaction

The streamlines of a fluid around the fiber are curved. Particles with finite mass and moving with the flow may not follow the streamlines exactly due to their inertia. If the curvature of a streamline is sufficiently large and the mass of a particle is sufficiently high, the particle may deviate far enough from the streamline to collide with the media surface as shown in Fig. 2.10 (Hinds, 1999). The importance of this inertial impaction mechanism increases with increasing particle size and increasing air velocity, as shown in Fig. 2.8. Therefore, the effect of increasing air velocity on the inertial impaction of particles is contrary to that for the diffusive deposition. The inertial impaction mechanism can be studied by the use of the dimensionless Stoke number (*Stk*), defined as

$$Stk = \frac{\rho_p d_p^2 C_c U_0}{18 \mu_g d_f} \tag{2-24}$$

The Cunningham correction factor is defined as

$$C_c = 1 + \frac{2.52\lambda}{d_p} \qquad \text{for } d_p = 0.1 \text{ μm} \tag{2-25}$$

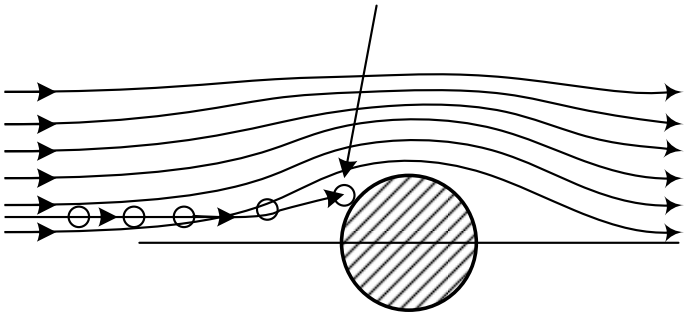

Figure 2.10 Single-fiber collection of a particle by inertial impaction.

The Stoke number is the basic parameter describing the inertial impaction mechanism for particle collection in a filter. A large Stoke number implies a higher probability of collection by impaction, whereas a small Stoke number indicates a low probability of collection by impaction.

The expression for the single-filter filtration efficiency due to inertial impaction (η_{imp}), using the Kuwabara flow field was proposed by Stechinna et al. (1969):

$$\eta_{imp} = \frac{(Stk)J}{(2Ku)^2} \tag{2-26}$$

$$J = (29.6 - 28\alpha_f^{0.62})R^2 - 27.5R^{2.8} \quad \text{for} \quad R < 0.4 \tag{2-27}$$

For approximate analysis, a value of $J = 2$ for $R > 0.4$ can be used.

Gravitational Settling

Particles will settle with a finite air velocity in a gravitational force field. When the settling velocity is sufficiently large, the particles may deviate from the gas streamline. Under downward filtration conditions, this would cause an increased collection due to gravity. When flow is upward, this mechanism causes particles to move away from the collector, resulting in a negative contribution to filtration. This mechanism is important only for particles larger than at least a few micrometers in diameter and at low air velocity. The dimensionless parameter governing the gravitational sedimentation mechanism is

$$Gr = \frac{V_g}{U_0} = \frac{\rho_g d_p^2 C_c g}{18\mu_g U_0} \tag{2-28}$$

where V_g is the settling velocity of the particle (m s^{-1}).

The single-fiber filtration efficiency due to gravity (η_{grav}) can be approximated as (Davies, 1973):

$$\eta_{grav} = \frac{Gr}{1+Gr} \tag{2-29}$$

CHAPTER 3
EXPERIMENT

In the present work, an appropriate lab-scaled test cyclone is constructed. The aerosol penetration (or collection efficiency) of the test cyclone for fine particles (0.3, 0.5 and 1.0 μm) and its reduction characteristic by an addition of filter (fibrous or stainless steel) to the annular space of the cyclone are studied. The penetration and pressure drop are investigated under laboratory conditions by varying parameters such as particle size, inlet velocity, filter types and filter configuration.

3.1 The Aerosol Collectors

3.1.1 Configuration of Original Cyclone Collector

The test cyclone in the present work is a reversed flow circular duct inlet type. It consists of four main parts: inlet, separation chamber, dust chamber and vortex finder. It was made of clear acrylic, and the dimensions are shown in Fig. 3.1 and Table 3.1. The same cyclone was used throughout this research work.

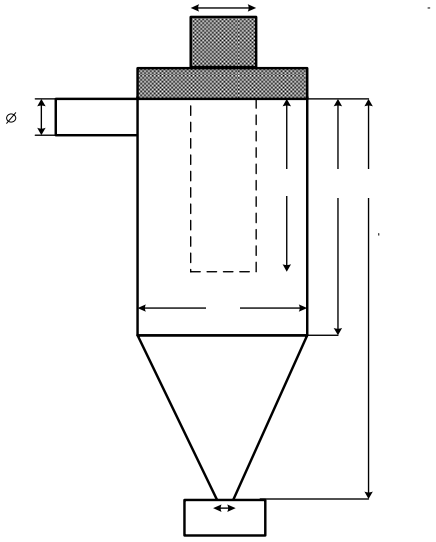

Figure 3.1 Dimensions of the test cyclone.

Table 3.1 Dimensions of test cyclone

Parameter	Dimension
Cyclone diameter, D_c (mm)	41
Outlet diameter, De (mm)	16
(with the wall thickness of 2 mm)	
Inlet diameter, ø (mm)	8
Outlet height, S (mm)	48
Cyclone height, H (mm)	109
Cylindrical body height, h (mm)	64
Cyclone dust outlet, B (mm)	6

3.1.2 Configuration of Combined Cyclone-Filter Collector

In order to reduce aerosol penetration (or enhance collection efficiency) of the cyclone, fibrous filter and stainless steel filter are chosen to combine with the cyclone. The configurations of combined cyclone-filter collectors are described below.

Combined Cyclone-Fibrous Filter Collector

The cyclone combined with fibrous filter is shown in Fig. 3.2 and its photograph is shown in Fig. 3.3. Four slabs of the fibrous filter are attached to the exit core as shown in the diagram. The thickness of the filter is 5 mm while the widths of the filter are set to 4 and 8 mm. Each filter is installed 90° apart. Under this configuration, the flow is perpendicular to the filters. When the 4 and 8-mm-width filters are attached, the gaps between the filter tip and the cyclone wall are 6 and 2 mm, respectively. The effect of the gap to the aerosol penetration will be studied. Physical properties of the fibrous filter are given in Table 3.2.

Table 3.2 Physical properties of the filters

Properties	Fibrous filter	Stainless steel filter
Fiber diameter, d_f (μm)	15.54	8.65
Thickness, Z (mm)	5	5
Packing density, α_f (-)	0.0396*	0.0065

* α_f is estimated from Davies' equation (Davies, 1952).

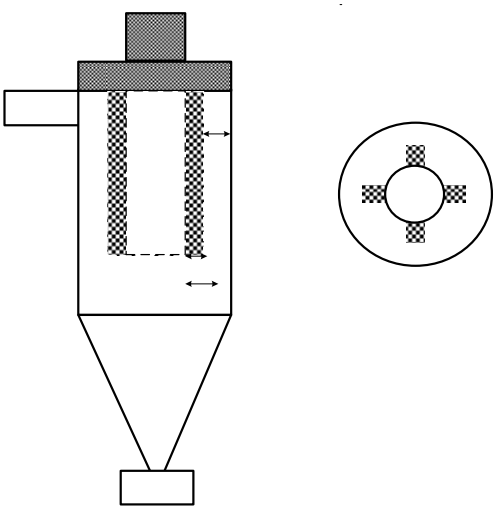

Figure 3.2 Diagram of combined cyclone-fibrous filter.

Figure 3.3 Photograph of cyclone combined with fibrous filter.

Combined Cyclone-Stainless Steel Filter Collector

The stainless steel filter used in this experiment is the inertial filter used by Otani et al. (2007) in the collection of nanoparticles. Properties of the filter are given in Table 3.2. When using the stainless steel filter, the configuration has been modified from the preceding setup. The space between the inner core and the wall of the cyclone has been filled with the filter as shown in Figs. 3.4 and 3.5. This is because the stainless steel filter can not be formed into the sheet as in the case of the fibrous filter. Two different amounts of stainless steel filter, 0.94 and 1.83 g are used.

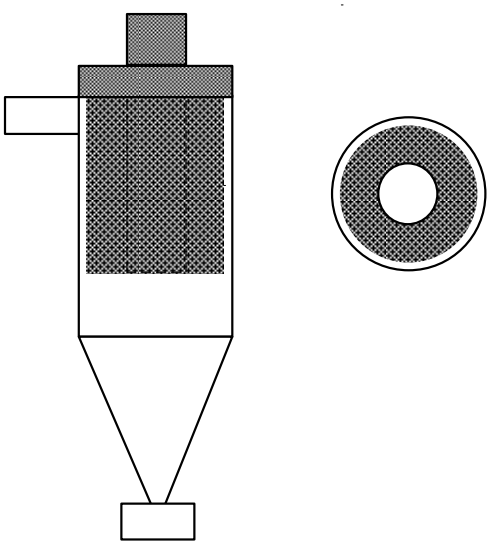

Figure 3.4 Diagram of combined cyclone-stainless steel filter.

Side view

Figure 3.5 Photograph of cyclone combined with stainless steel filter.

Physical Properties of the Filters

Physical properties of both filters are shown in Table 3.2. The properties of both fibrous filter and stainless steel filter are obtained from the manufactures of Bilin Company (Japan) and Top value Company (Japan), respectively. While the fiber diameters are obtained from the SEM images which are shown in Fig. 3.6.

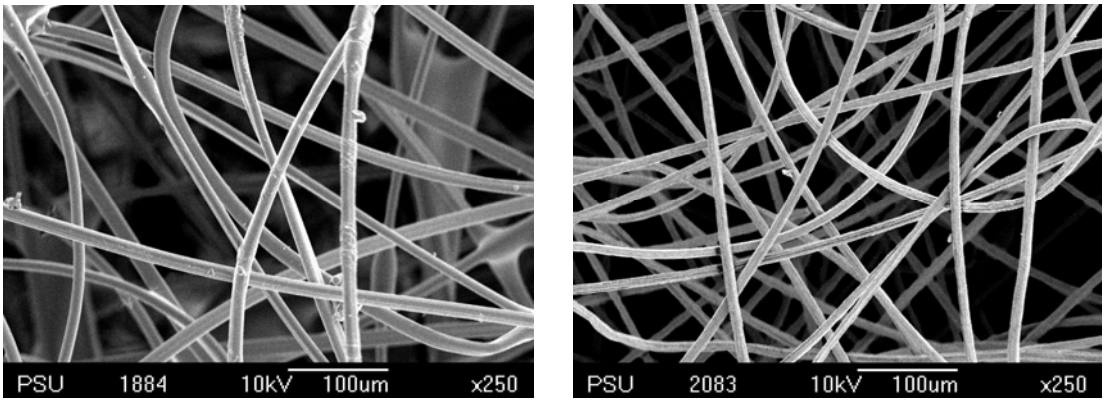

(a) (b)

Figure 3.6 SEM images of (a) fibrous filter and (b) stainless steel filter.

3.2 Experimental Setup

Schematic diagram of the experimental setup is shown in Fig. 3.7 and its photograph is shown in Fig. 3.8. The test aerosols were spherical polystyrene particles of diameters 0.3, 0.5 and 1.0 μm, generated from polystyrene latex (PSL) solution using a collision atomizer (TSI, Model 3079). Water vapor was removed from the atomized particles by passing the aerosol through a silica gel diffusion dryer. Then the dried polystyrene aerosol particles were diluted with cleaned air passing through an absolute filter (American Air Filter, Astrocel II). The particles were neutralized by Am-241 (Japan Radioactive Association) and then introduced into the aerosol collector. The desired flow rate or inlet velocity was controlled by adjusting the needle valves and measured by orifice meters and the corresponding U-tube

manometers. HEPA filter was used to prevent the aerosol particles from passing through the orifice meter during experiment.

The aerosol penetration and the pressure drop of the aerosol collectors were measured to evaluate the collection performance. The penetration was determined at various velocities for each particle size by measuring the number of particles at upstream and downstream of the aerosol collectors using a laser particle counter or LPC (Royco, Portable 330B). The LPC measures particle number concentration in five size ranges: ≥ 0.3 μm, ≥ 0.5 μm, ≥ 0.7 μm, ≥ 1.0 μm and ≥ 5 μm. The penetration (P) can then be calculated from

$$P = \frac{C_{outlet}}{C_{inlet}} \tag{3-1}$$

Here C_{inlet} and C_{outlet} are concentrations of particles at the upstream and downstream of the aerosol collectors. The pressure drop across the aerosol collectors was measured by either a differential pressure transducer (MSK, Baratron pressure transducer Type 223) or a U-tube manometer.

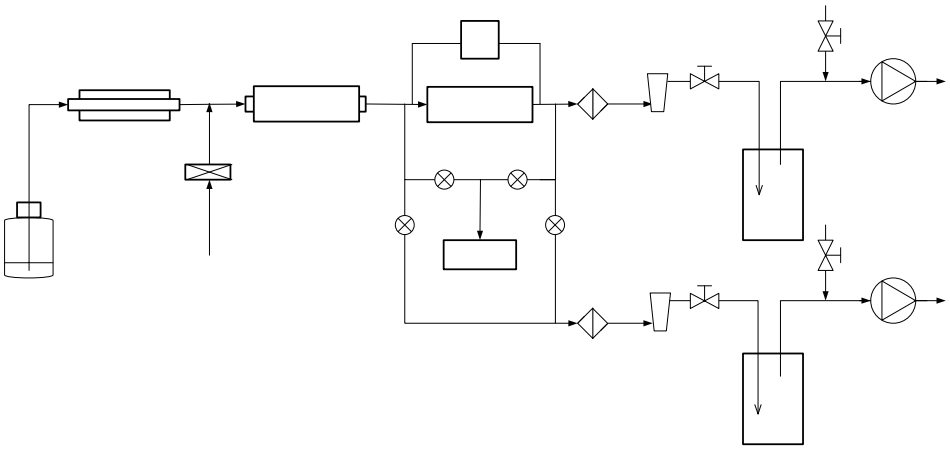

Figure 3.7 Schematic diagram of the experimental setup for measuring collection efficiency of the aerosol collectors.

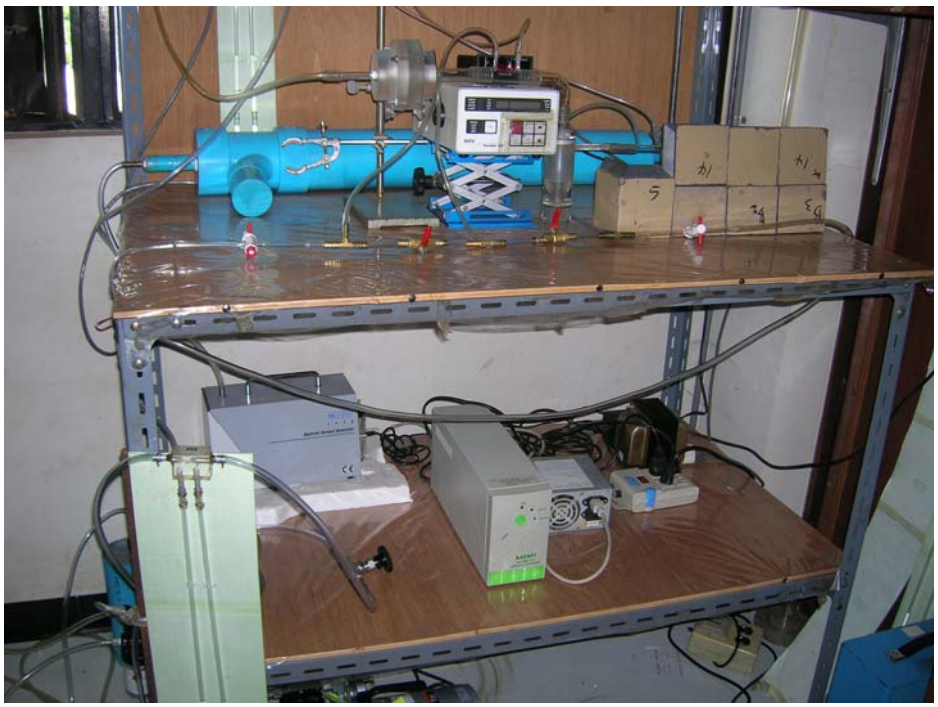

Figure 3.8 Photograph of the experimental setup.

Experimental Parameters

The aerosol collection performance of the original cyclone and the combined cyclone-filter collectors were investigated by varying basic operating parameters such as particle size, inlet velocity and filter types as given in Table 3.3.

Table 3.3 Parameters used in the experiment

Condition	Range
Particle size, d_p (μm)	0.3, 0.5 and 1.0
Inlet velocity, U (m s^{-1})	1.84, 3.53, 4.09, 5.78, 8.53, 13.45 and 16.72
Fibrous filter width (mm)	4 and 8
Amount of stainless steel (g)	0.94 and 1.83

3.3 Preparation of Polystyrene Latex

The polystyrene particle sizes of 0.3 and 0.5 μm are obtained from Duke scientific. Polystyrene particle size of 1.0 μm was prepared by soap-free emulsion polymerization (Inukai et al., 2001). A 250 mL three-necked flask was purged with nitrogen gas. Then 22.9 g of styrene (99.9% wt., Merck), 0.35 g of NH_4OH (35% min., J.T.Baker) and 0.05 g of NH_4Cl (Analytical-grade, J.T.Baker) were charged into the flask. The volume was adjusted by adding deionized water and reaction mixture was deoxygenated by bubbling with nitrogen gas under stirring. After heating the reactant to 65°C, 3.14 g of 2,2′-azobis[*N*-(2-carboxyethyl)-2,2-methylpropionamidine] *n*-hydrate initiator (95.0% min, Wako Pure Chemical) was added. When monomer droplets disappeared (after 10 h of reaction time), polystyrene particles were precipitated by pouring the reaction mixture into excess methanol (Analytical-grade, J.T.Baker), and collected by filtration. The size distribution of polystyrene particles was measured using laser particle analyzer (Malvern, Mastersizer 2000) as shown in Fig 3.9. The volume-averaged diameter of the particles was 2.2 μm while the coefficient of variation was 189.3 %. The obtained particles were dispersed in 0.5% sodium docecylsulphate (SDS) solution and centrifuged. Then the upper fraction was collected and redispersed again in 0.5% SDS, then used in this work.

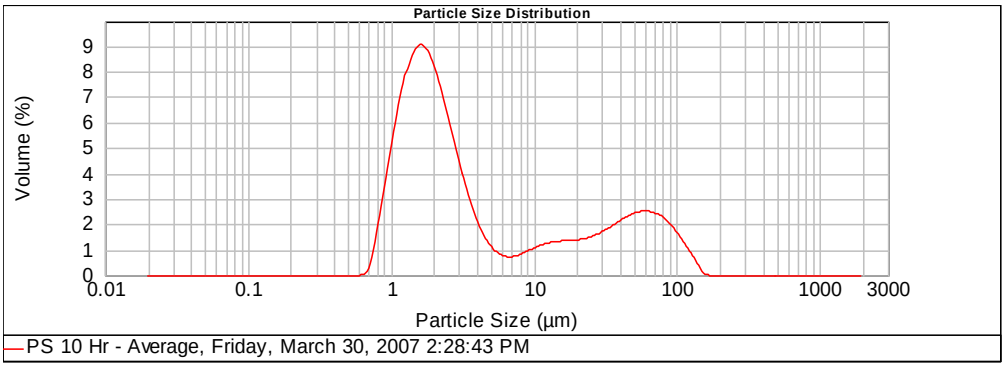

Figure 3.9 Particle size distribution of polystyrene particles.

CHAPTER 4

RESULTS AND DISCUSSION

4.1 Aerosol Penetration of the Test Cyclone

The penetration of a model cyclone collector was investigated for fine particle sizes of 0.3, 0.5 and 1.0 μm. The experimental results were compared with three models: Crawford (1976), mixed flow (de Nevers, 1995) and Leith and Licht (1972) models as shown in Figs. 4.1 (a), (b), (c) and (d), for inlet velocities of 1.84, 4.09, 8.53 and 16.72 m s^{-1}, respectively. It appears that the Crawford model gives the best agreement with experimental results for all inlet velocities. That means the effect of the turbulent eddies results in the lowering of the tangential velocity so that the actual velocity distribution follows rather closely the modified cyclone-flow distribution of Eq. (2-5). However, for inlet velocity of 1.84 m s^{-1}, the deviation from the mixed flow model is not very large. The agreement with the Crawford model is not surprising as it was carried out to calculate the particle collection efficiency for the reverse flow cyclone. Leith and Licht model is based on the assumptions of a force balance showing the lower calculated penetration than the other models (Lorenz et al, 1994). The differences between penetration calculated from Crawford model and experimental results for each particle size of all velocities are shown in Table 4.1.

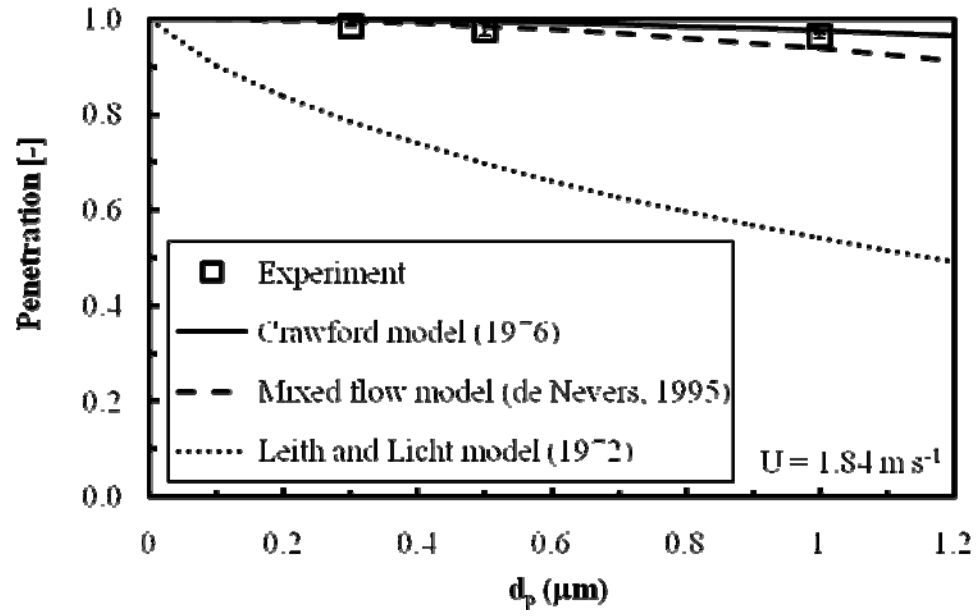
Penetration [-]
1.0
0.8
0.6
0.4
0.2
0.0
0
0.2
0.4
0.6
0.8
1
1.2
d_p (μm)
Experiment
Crawford model (1976)
Mixed flow model (de Nevers, 1995)
Leith and Licht model (1972)
U = 1.84 m s^{-1}

(a)

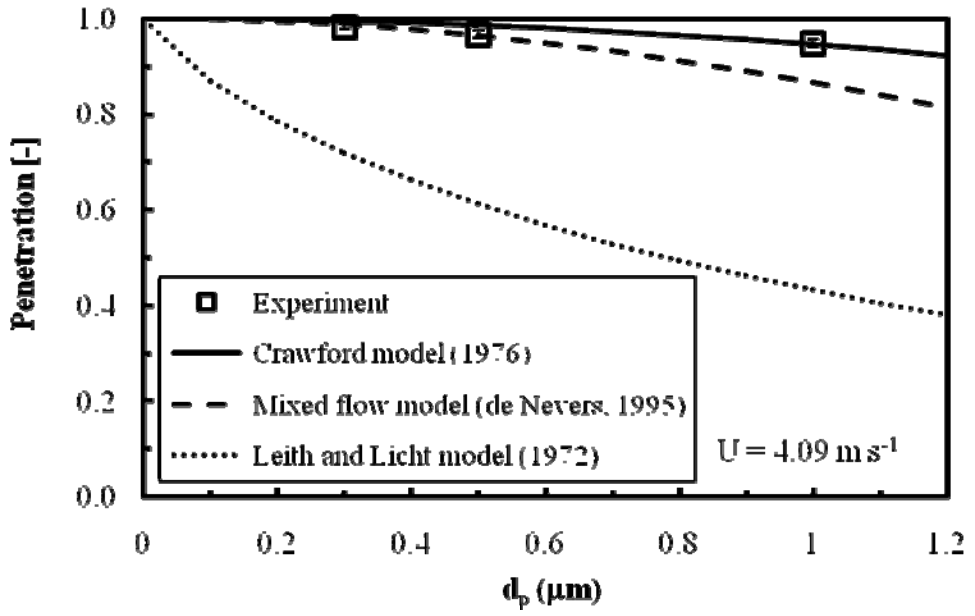
Penetration [-]
1.0
0.8
0.6
0.4
0.2
0.0
0
0.2
0.4
0.6
0.8
1
1.2
d_p (μm)
Experiment
Crawford model (1976)
Mixed flow model (de Nevers, 1995)
Leith and Licht model (1972)
U = 4.09 m s^{-1}

(b)

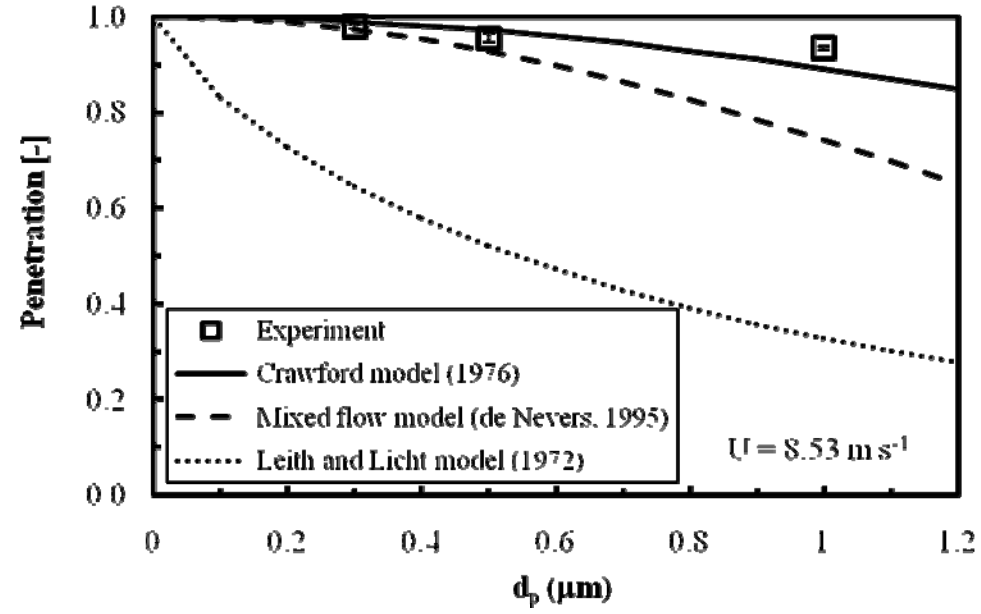

(c)

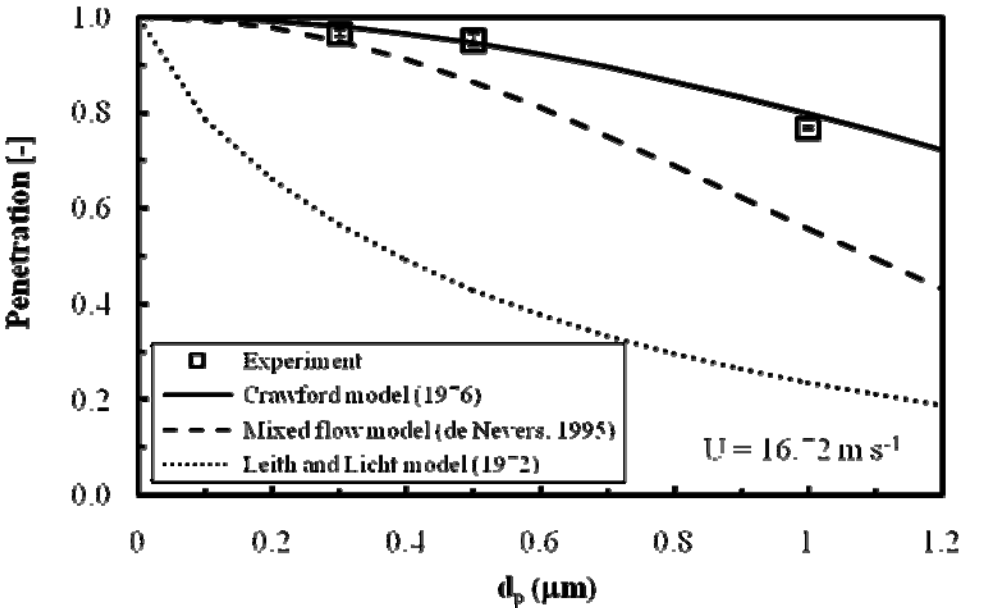

(d)

Figure 4.1 Comparison between theoretical and experimental data of dust penetration at inlet velocities of (a) 1.84 m s^{-1}, (b) 4.09 m s^{-1}, (c) 8.53 m s^{-1} and (d) 16.72 m s^{-1}.

Table 4.1 The differences between the penetration calculated from Crawford model and experimental results

Inlet velocity, m s^{-1}	% Difference		
		d_p = 0.5 μm	d_p = 1.0 μm
1.84	1.27	1.72	1.14
3.53	1.24	2.08	0.5
4.09	1.25	1.89	0.25
5.78	1.14	1.26	1.7
8.53	0.95	1.68	4.87
13.45	0.91	0.15	0.92
16.72	1.45	0.65	3.78
average	1.17	1.35	1.88

4.2 Collection Efficiency of the Combined Cyclone-Filter Collectors

The aerosol penetration of the combined cyclone-filter collector was investigated, and compared with that of the test cyclone**.** The effecting parameters include particle size and the gap between fibrous filters and the cyclone wall.

4.2.1 Effect of Particle Size for the Combined Cyclone-Fibrous Filter Collector

The effect of particle size (0.3, 0.5 and 1.0 μm) on the penetration of the combined cyclone-fibrous filter collectors was investigated and compared with the model cyclone for 4 different inlet velocities: 1.84, 4.09, 8.53 and 16.72 m s^{-1}, as shown in Figs. 4.2 (a) to (d). It was found that the penetration of cyclone and

combined cyclone-filter collectors decreases significantly when either particle size or gas inlet velocity increases. In the case of combined cyclone-fibrous filter collector, when fibrous filter width increases, the penetration decreases. Penetration for the cyclone combined with 4-mm-width filter is lowered by 0.4-2.2%, 0.6 – 6.2% and 3.2 – 9.4% from that of the cyclone alone for the particle sizes of 0.3, 0.5 and 1.0 μm, respectively, in the tested velocity range. The values for the cyclone combined with 8-mm-width filter are 0.3 – 5.5%, 1.3 – 15.8% and 1.7 – 19.9% in the same tested velocity range. The presence of the fibrous filter enhances the collection efficiency of fine particles via changing the centrifugal force to inertial impaction. The filtration mecahnism becomes more significant for collecting the fine particles. For filtration, the penetration of fine particles was calculated from equation (2-22) for fibrous filter and shown in Fig. 4.3. From this figure, it can be seen that the penetration decreases with increasing the particle size and filtration velocity. However, at inlet velocity of 16.72 m s^{-1} and fibrous filter width of 4 mm, the penetration is higher than that of the cyclone for the particle size of 1.0 μm. This is because the cyclone flow field was disturbed by the filters, similar to the results of Wang et al. (2005). They reported that the insertion of the stick into the cyclone changed the cyclonic flow distribution by decreasing the tangential velocity and increasing the turbulence intensity. Therefore, the particle size of 1.0 μm caused a higher penetration due to its trajectory was disturbed by fibrous filters, while the smaller sizes were collected by the filter.

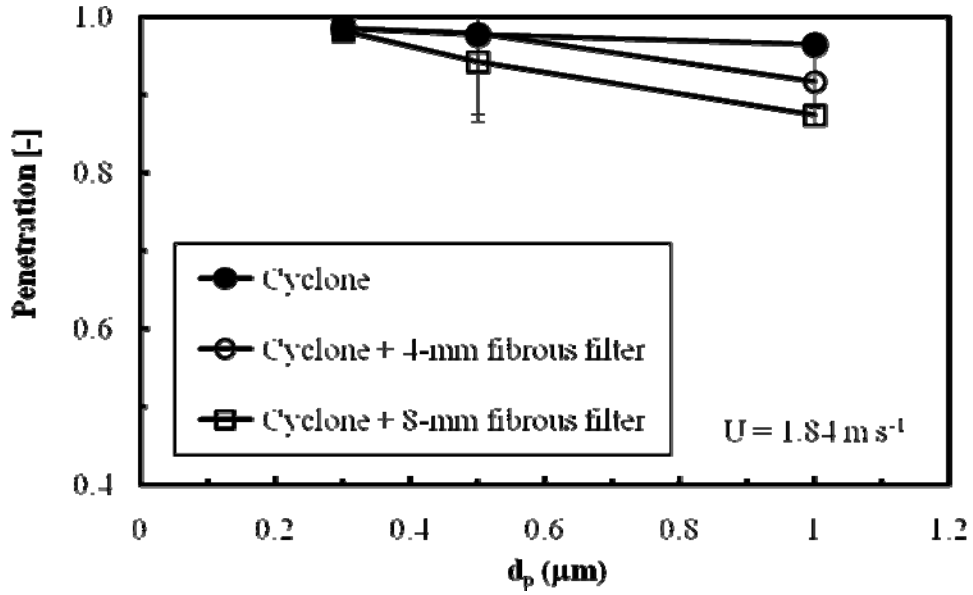
1.0
0.8
0.6
0.4
Penetration [-]
0
0.2
0.4
0.6
0.8
1
1.2
d_p (μm)
Cyclone
Cyclone + 4-mm fibrous filter
Cyclone + 8-mm fibrous filter
U = 1.84 m s^{-1}

(a)

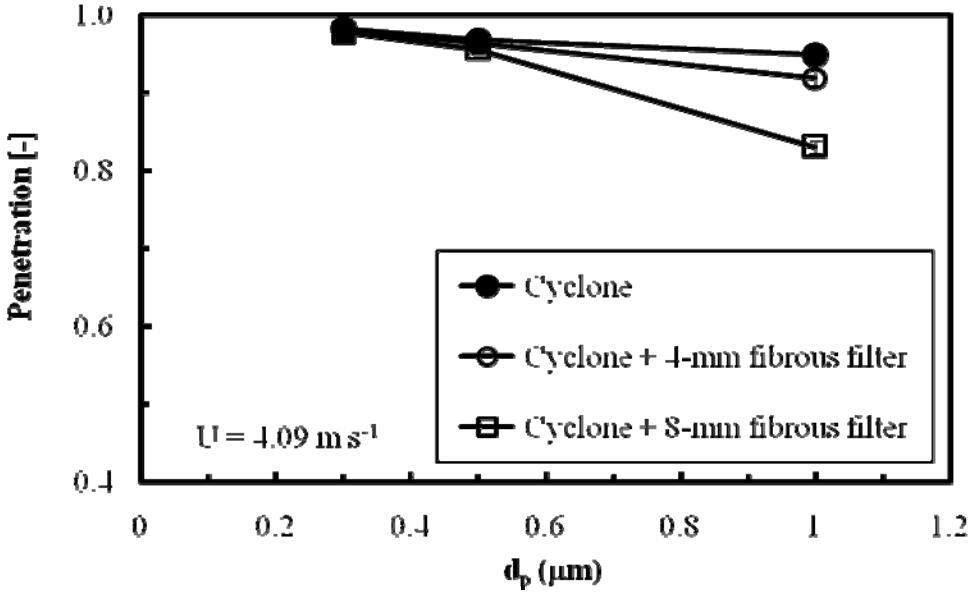
1.0
0.8
0.6
0.4
Penetration [-]
0
0.2
0.4
0.6
0.8
1
1.2
d_p (μm)
Cyclone
Cyclone + 4-mm fibrous filter
Cyclone + 8-mm fibrous filter
U = 4.09 m s^{-1}

(b)

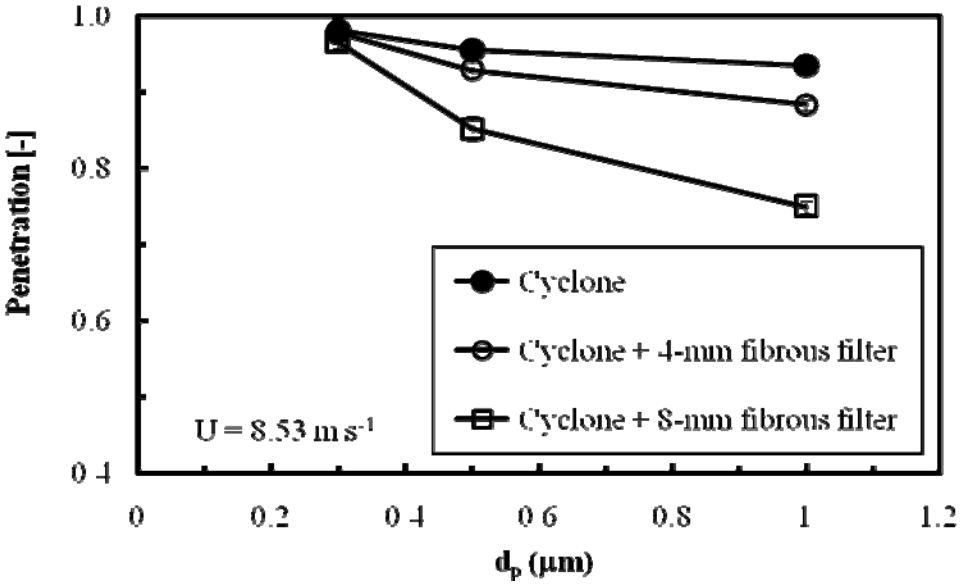

(c)

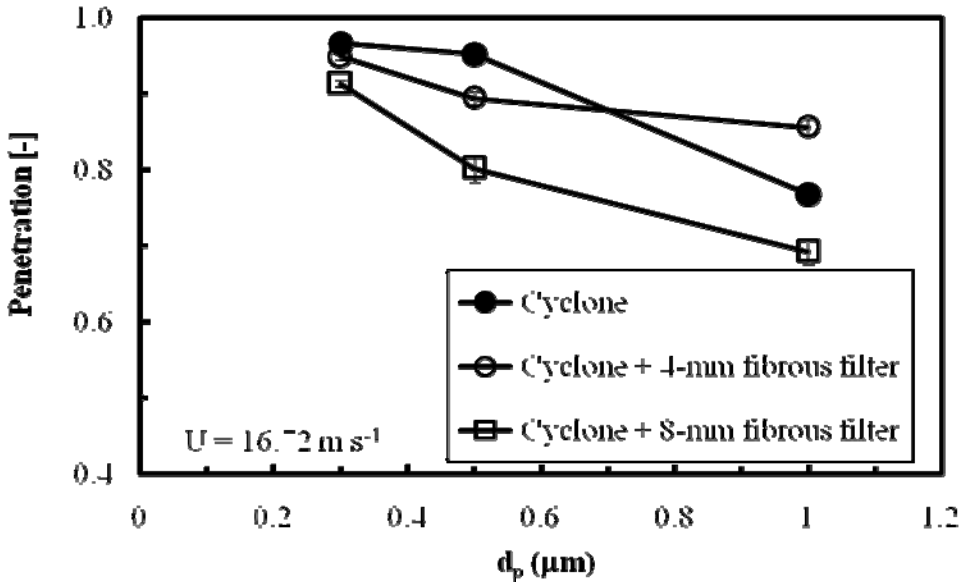

(d)

Figure 4.2 The effect of particle size on the penetration for the combined cyclone-filter collector at inlet velocities of 1.84 m s^{-1}, (b) 4.09 m s^{-1}, (c) 8.53 m s^{-1} and (d) 16.72 m s^{-1}.

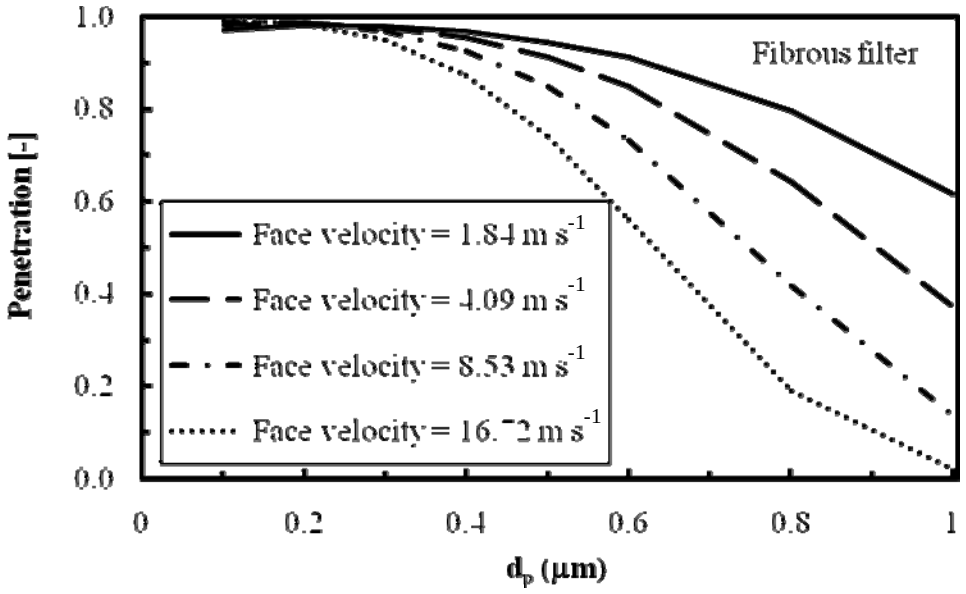

Figure 4.3 The effect of particle size on the penetration for filtration with fibrous filter at inlet velocities of (a) 1.84 m s^{-1}, (b) 4.09 m s^{-1}, (c) 8.53 m s^{-1} and (d) 16.72 m s^{-1}.

4.2.2 Effect of the gap between filter tip and the cyclone wall to the collection efficiency

The gaps between fibrous filter tip and cyclone wall are 6.5 and 2.5 mm for cyclone combined with fibrous filter of 4 mm and 8 mm width, respectively. The penetration of the combined cyclone-filter collector tends to decrease with increasing the filter width or reducing the gap. This is due to the greater filtration area for the larger filter. The larger width of the attached filter reduces the area of the spiral flow. The layer of the flow away from the cyclone wall contains smaller particles than the layer near the wall. This could be why the small particle collection efficiency increases for the combined cyclone filter collector.

4.2.3 Effect of Particle Size for the Combined Cyclone-Stainless Steel Filter Collector

The combined cyclone-filter collector was modified by changing the filter type to stainless steel filter. In this experiment the filter material was used to fill up the annular space between the cyclone wall and the exit core. The effect of particle size on the penetration of the combined cyclone-stainless steel filter collector compared with the original cyclone for 4 different inlet velocities are shown in Figs. 4.4 (a) to (d). The results show that the penetration of the combined cyclone-stainless steel filter collector decreases with increasing the amount of the filter as expected. Besides, the penetration of the cyclone combined with stainless steel filter collector also decreases with increasing the particle sizes. When the cyclone combined with 0.94 g stainless steel filter, the penetration is lowered by 0.6 – 4.7%, 0.8 – 13.7%, 1.1 – 20.9% for particle sizes of 0.3, 0.5 and 1.0 μm, respectively, from that of the cyclone in the tested velocity range. When the amount of filter is double to 1.83 g, these values are 3.7 – 14.8%, 4.3 – 31.2%, 11.6 – 41.2%. The explanation for this is similar to the case of the combined cyclone-fibrous filter. The penetration for filtration using stainless steel filter, calculated from the equation of (2-22), is shown in Fig. 4.5.

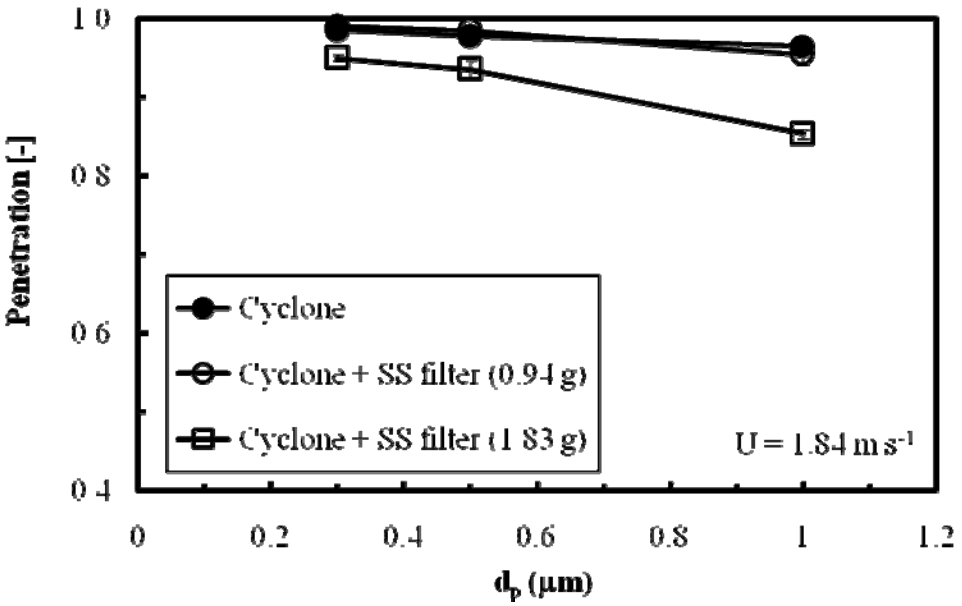
1.0
0.8
0.6
0.4
Penetration [-]
0
0.2
0.4
0.6
0.8
1
1.2
d_p (μm)
Cyclone
Cyclone + SS filter (0.94 g)
Cyclone + SS filter (1.83 g)
U = 1.84 m s^{-1}

(a)

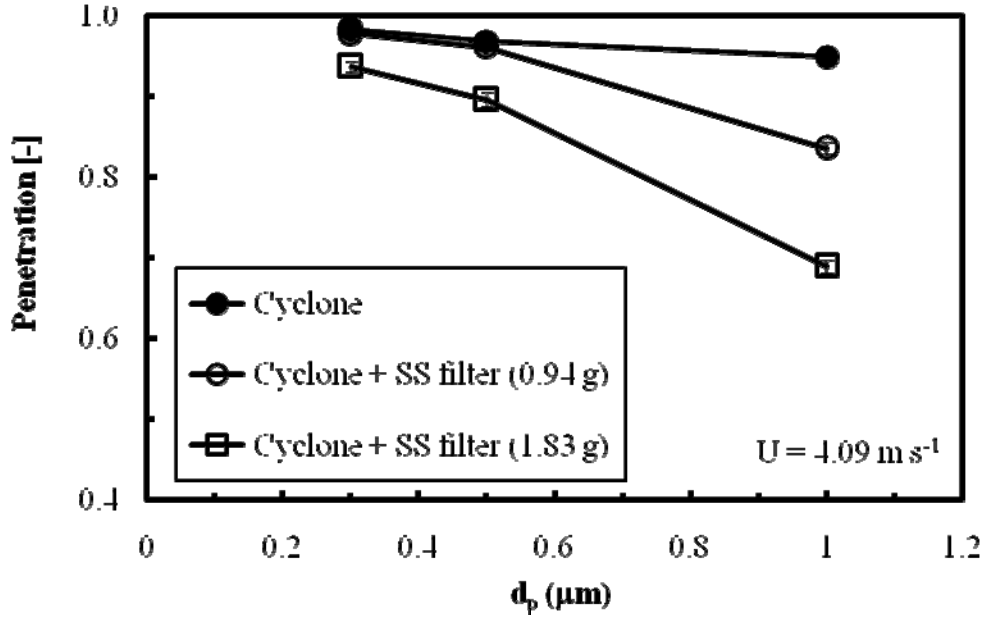
1.0
0.8
0.6
0.4
Penetration [-]
0
0.2
0.4
0.6
0.8
1
1.2
d_p (μm)
Cyclone
Cyclone + SS filter (0.94 g)
Cyclone + SS filter (1.83 g)
U = 4.09 m s^{-1}

(b)

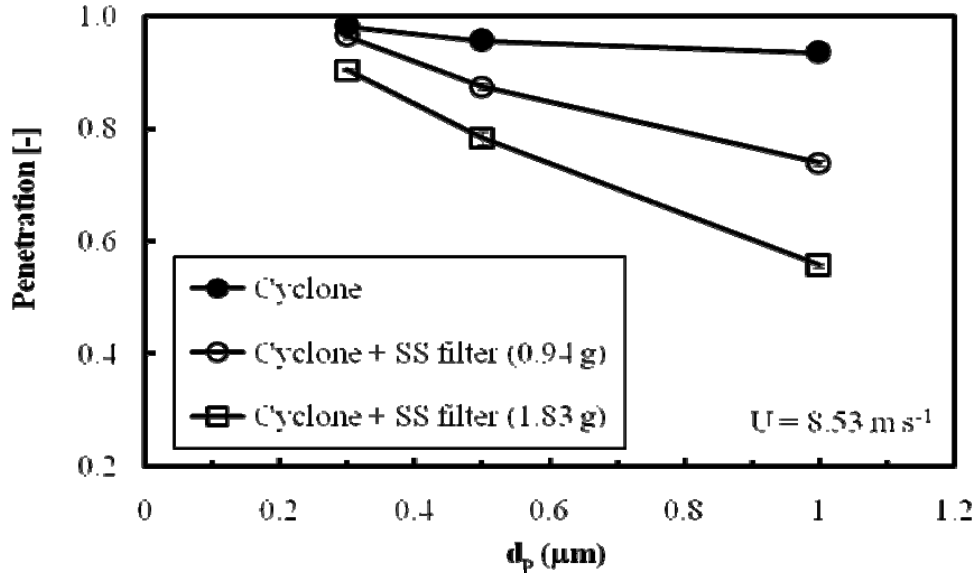

(c)

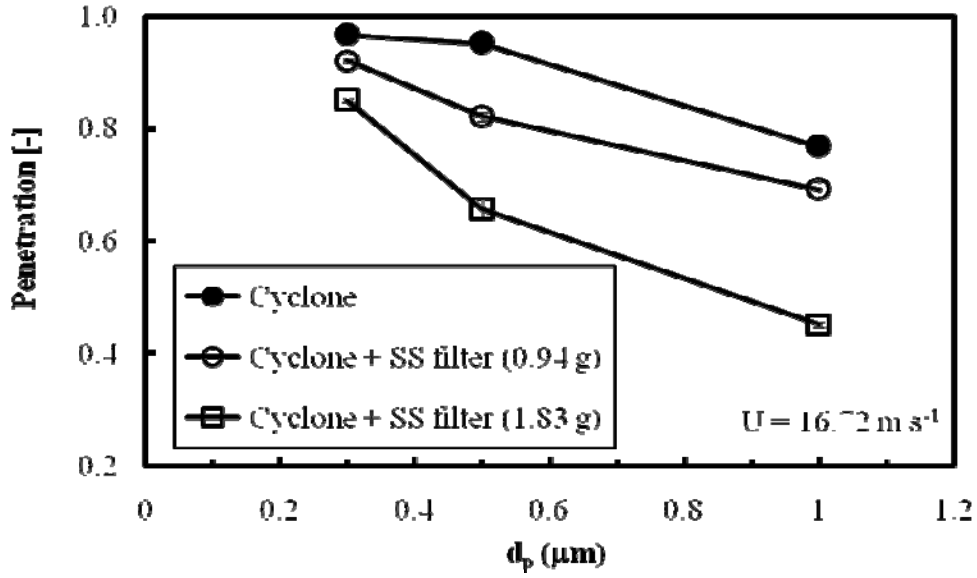

(d)

Figure 4.4 The effect of particle size on the penetration for the combined cyclone-stainless steel filter collector at inlet velocities of 1.84 m s^{-1}, (b) 4.09 m s^{-1}, (c) 8.53 m s^{-1} and (d) 16.72 m s^{-1}.

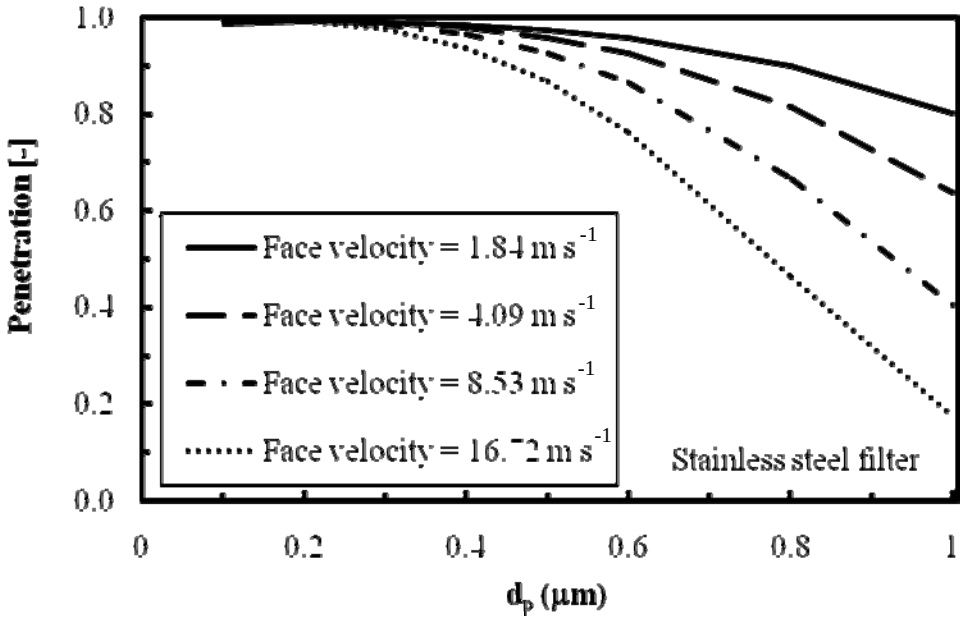

Figure 4.5 The effect of particle size on the penetration for filtration with stainless steel filter at inlet velocities of 1.84 m s^{-1}, (b) 4.09 m s^{-1}, (c) 8.53 m s^{-1} and (d) 16.72 m s^{-1}.

4.3 Pressure drop

4.3.1 Pressure Drop Prediction under Different Inlet Velocities

The cyclone pressure drop was measured for inlet velocity ranging from 1.84 to 16.72 m s^{-1}. The comparison between experimental data and theoretical calculation is shown in Fig. 4.6. The results show that Dirgo's model (Dirgo, 1988) yields a best prediction of cyclone pressure drop under different operated inlet velocities with the errors of 2.7 – 54.4%. Since the pressure drop coefficient (α) for Dirgo's model includes the other dimensions of cyclone (Karagoz and Avci, 2005).

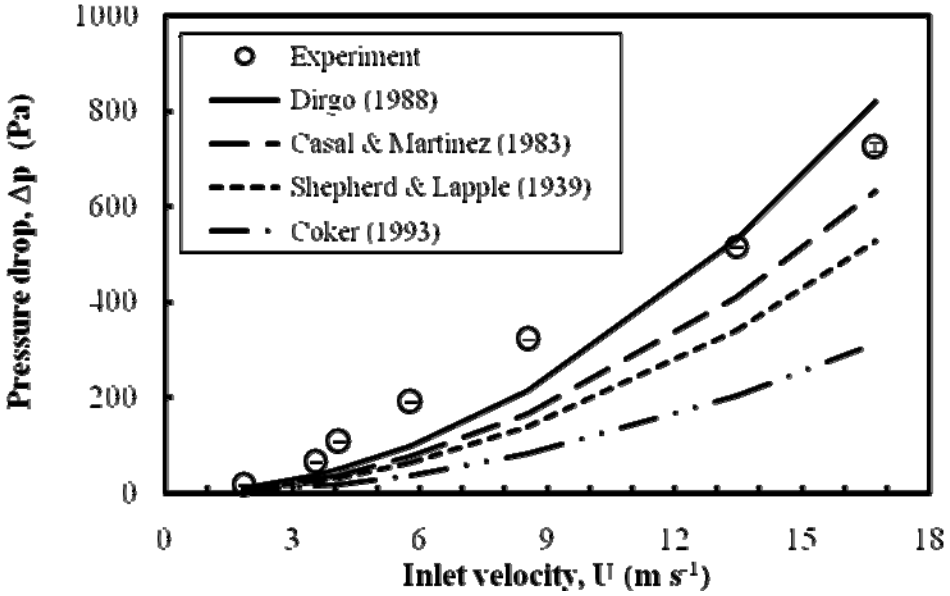

Figure 4.6 Evolution of cyclone pressure drop with inlet velocity and a comparison between experimental data and four empirical models.

4.3.2 Pressure Drop of the Combined Cyclone-Filter Collector

Fig. 4.7 shows that the pressure drop of combined cyclone-filter collectors is smaller than that of cyclone. This is due to the presence of the filter causes the increasing of the turbulence intensity affecting in the reduction of tangential velocity (Wang et al. 2005). For the cyclone combined with fibrous filter 4-mm and 8-mm-width, the pressure drop is lower by 32.7 and 38.8%, respectively. The flow is perpendicular to the filters and the flow field is disturbed by the filters, cause the decrease of velocity. When cyclone combined with 0.94 g and 1.83 g of stainless steel filter, the pressure drop is lower by 23.5 and 20.2% respectively. The pressure drop reduction of cyclone combined with 0.94 g of stainless steel filter is lower than that of cyclone combined with 1.83 g of stainless steel filter. That because of the reduction of annular space increases the tangential velocity.

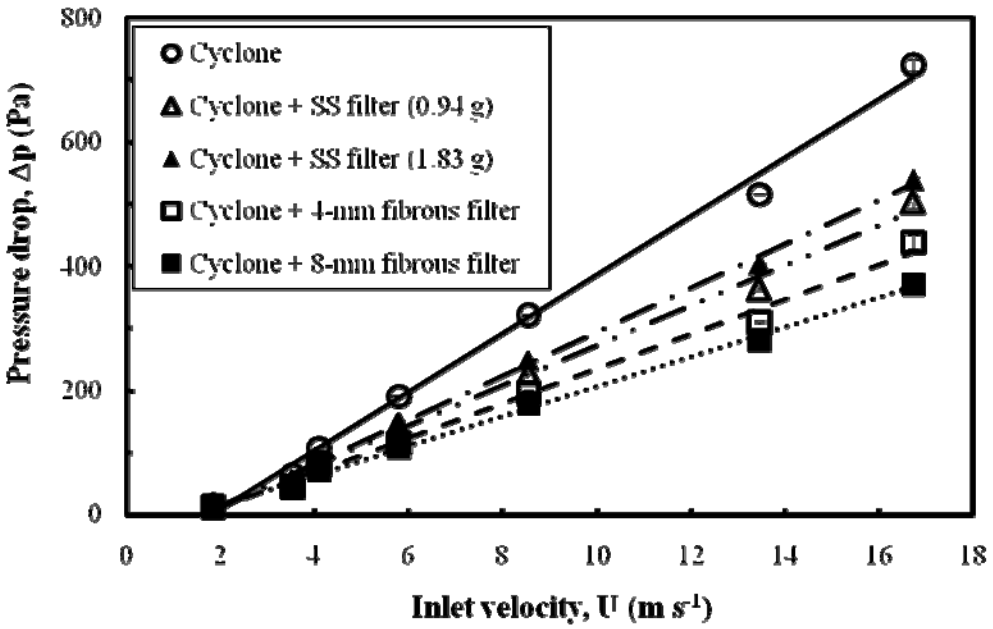

Figure 4.7 The relationship between the pressure drop and velocity for cyclone and combined cyclone–filters collectors.

CHAPTER 5
CONCLUSIONS

In this work the fine dust collection performance of the test cyclone collector was improved by the cyclone-filter combination. The penetration characteristics of the test cyclone, filter, cyclone-filter collectors for the fine particles were studied. Moreover, types and configuration of filters were investigated. The following conclusions can be drawn from the present study:

(1) The theoretical values are in an acceptable agreement with experiment results for the normal cyclone. Average values of difference between theoretical penetration and experimental results of cyclone performance for particle of 0.3, 0.5, 1.0 μm are 1.47%, 1.76% and 2.21% respectively, in the test velocity range.

(2) The penetration of a cyclone and a combined cyclone-filter collectors decrease with increasing either particle size or inlet velocity as expected.

(3) The penetration of a combined cyclone-filter collector with 4-mm-width fibrous filter is lower by 0.4 – 2.2%, 0.6 – 6.2% and 3.2 – 9.4% than that of original cyclone for the particle sizes of 0.3, 0.5 and 1.0 μm, respectively, in the test velocity range. However, at inlet velocity of 16.72 m s^{-1} the penetration of the combined cyclone-filter is higher than original cyclone for the particle size of 1.0 μm. This is due to the cyclone flow field was disturbed by presence of the filter.

(4) The penetration of a combined cyclone-filter with 8-mm-width is lower by 0.3 – 5.5%, 1.3 – 15.8% and 1.7 – 19.9% than that for original cyclone of the particle sizes of 0.3, 0.5 and 1.0 μm, respectively, in the test velocity range.

(5) The penetration of a combined cyclone-filter collector with 0.94 g of stainless steel is lower by 0.6 – 4.7%, 0.8 – 13.7%, 1.1 – 20.9% than

that of original cyclone for the particle sizes of 0.3, 0.5 and 1.0 μm, respectively, in the test velocity range.

(6) The penetration of a combined cyclone-filter with 1.83 g of stainless steel is lower by 3.7 – 14.8%, 4.3 – 31.2%, 11.6 – 41.2% than that of original cyclone for the particle sizes of 0.3, 0.5 and 1.0 μm, respectively, in the test velocity range.

(7) The penetration of fibrous filter and stainless steel filter in filtration tends to decrease with increasing face velocity. This is because the dominance of interception or impaction when the velocity is increased.

(8) The pressure drop of cyclone combined with 4-mm and 8-mm fibrous filter width at the same inlet velocities is lower than cyclone pressure drop about 32.7 and 38.8%, respectively.

(9) The pressure drop of combined cyclone-stainless steel filter, which amount of stainless steel filter are 0.94 and 1.83 g at the same inlet velocities is lower than cyclone pressure drop about 23.5, 20.2% respectively.

(10) The pressure drop of fibrous filter and stainless steel filter in filtration at the same inlet velocities is higher than cyclone pressure drop about 630% and 360% respectively.

REFERENCES

Avci, A.; Karagoz, I. “Effects of flow and geometrical parameters on the collection efficiency in cyclone separators” *J. Aerosol Sci.* **2003**, *34, 937*-955.

Arthur, C.S. *Air pollution*, 2th ed., Academic Press Inc., New York, 1968.

Antony, J.B.; Wayne, T.D. *Air pollution Engineering Manual*, VAN NOSTRAND REINHOLD PRESS Inc., New York, 1992.

Baron, P.A.; Willeke, K. *Aerosol Measurement: principles techniques and applications*, 1st ed., Van Nostrand Reinhold, New York, 1994.

Casal, J.; Martinez-Benet, J.M. “A better way to calculate cyclone pressure drop” *Chem. Eng.* **1983**, *90*, 99-100.

Chen, J., Lu, X., Liu, H. and Yang, C. (2006). Effect of the bottom-contracted and edge-sloped vent-pipe on the cyclone separator performance. *Chem. Eng. J.* J90: 99-100.

Crawford, M. *Air Pollution Control Theory*, 2nd ed., McGraw-Hill Inc., New Delhi. 1976.

Columbus, E.P.. “Series Cyclone arrangements to Reduce Gin Emissions” *Trans. of ASAE*. **1993**, *36(2)*, 545-550.

Coker, A.K.“Understand cyclone design” *Chem. Eng. Progress.* **1993**, *28*, 51-55.

Davies, C.N. The separation of airborne dust and particulates, *Proc. IMechE 1B.* 1952, 185-213.

Davies, C.N. *Air Filtration*, Academic Press, London, 1973.

Dirgo, J. Relationships between cyclone dimensions and performance, Doctoral Thesis, Havard University, USA, 1988.

Faith, W.L. *Air Pollution*, 2nd ed., John Wiley & Sons, Inc., New York, 1972.

Fassani, F.L.; Goldstein, L.Jr. "A study of the effect of high inlet solids loading on a cyclone separator pressure drop and collection efficiency" *Powder Technol.* **2000**, *107*, 60-65.

Gimbun, J.; Chuah, T.G.; Fakhru'l-Razi, A.; Choong-Thomas, S.Y. "The influence of temperature and inlet velocity on cyclone pressure drop: a CFD study" *Chem. Eng. Process.* **2005**, *44*, 7-12.

Hinds, W.C. *Aerosol Technology*, 2nd ed., John Wiley & Sons, Inc., New York, 1999.

Huang, S.H.; Chen, C.W.; Chang, C.P.; Lai, C.Y.; Chen, C.C. "Penetraion of 4.5 nm to 10μm aerosol particles through fibrous filters" *J. Aerosol Sci.* **2007**, *38*, 719-727.

Inukai, S.; Tanma, T.; Orihara, S. and Konno, M. "A simple method for producing micron-sized, highly monodisperse polystyrene particles in aqueous media: effect of impeller speed on particle size distribution" *Trans IChemE*. **2001**, *79*, 901-905.

Jiao, J.; Zheng, Y.; Sun, G.; Wang,J. "Study of the separation efficiency and the flow field of a dynamic cyclone" *Sep. Purification Technol*. **2006**, *49*, 157-166.

Jo, Y., Tien, C. and B.R. Madhumita. Development of a post cyclone to improve the efficiency of reverse flow cyclones. *Powder Technol*. **2000**,*113*, 97-108.

Jolius, G.; Chuah, T.G.; Fakhru'l-Razi, A.; Choong Thomas, S.Y. "The influence of temperature and inlet velocity of cyclone pressure drop: a CFD study" *Chem. Eng. Process.* **2005**, *44*, 7-12.

Karagoz, I. and Avci, A. "Modelling of the pressure drop in tangential inlet cyclone separators" " *Aerosol Sci. Tech.* **2005**, *39*, 857-865.

Kim, J.C.; Lee, K.W. "Experimental study of particle collection by small cyclone" *J. Aerosol Sci.* **1990**, *12*, 1003-1015.

Lapple, C.E. Air Pollution Engr. Manual, J.A. Danielson, ed., U.S. Dept. of Health, Education, &Welfare, Public Health Service Pub., No. 999-AP-40, 1967, 95.

Leith, D.; and Licht, W. "The collection efficiency of cyclone the particle collectors-a new theoretical approach", *AIChE Symp. Ser.* **1972**, *68*, 196–206.

Lee, J.W.; Yang, H.J.; Lee, D.Y. "Effect of the cylinder shape of a long-coned cyclone on the stable flow-field establishment" *Powder Technol.* **2006**, *165*, 30-38.

Lee, K.W. and Liu, B.Y.H. "Theoretical study of aerosol filtration by fibrous filters" *Aerosol Sci. Tech.* **1982**, *1* , 147-161.

Lim, K.S.; Kwon, S.B.; Lee, K.W. "Characteristics of the collection efficiency for a double inlet cyclone with clean air" *J. Aerosol Sci.* **2003**, *34*, 1085-1095.

Lim, K.S.; Kim, H.S.; Lee, K.W. "Comparative performances of conventional cyclones and a double cyclone with and without an electric field" *J. Aerosol Sci.* **2004**, *35*, 103-116.

Lim, K.S.; Kim, H.S.; Lee, K.W. "Characteristics of the collection efficiency for a cyclone with different vortex finder shapes" *J. Aerosol Sci.* **2004**, *35*, 743-754.

de Nevers, N. *Air Pollution Control Engineering*, 1st ed., McGraw-Hill Inc., New York, 1995.

Otani, Y.; Eryu, K.; Furuuchi, M.; Tajima, N.; Tekasakul, P. "Inertial classification of nanoparticles with fibrous filters" *Aerosol Air Qual. Res.***2007**, *7*, 343-352.

Othmer,K. *Encyclopedia of chemical technology*, 3rd ed., McGraw-Hill Book Co., New York, 1978.

Qian, F.; Zhang, J.; Zhang, M. "Effects of the prolonged vertical tube on the separation performance of a cyclone" *J. Hazardous Materials.* **2006**, *B136*, 822-829.

Stechkina, I. B.; Kirsch,A.A. and Fuch, N.A. "Study in fibrous aerosol filter-IV" *Ann. Occup. Hyg*. **1969**, *12*, 1-8.

Shepherd, C.B.; Lapple, C.E. *Air pollution control: a design approach*, 2nd ed., Woveland Press Inc., Illinois, 1939, 127-139.

Stern, C(Ed.). *Air Pollution*, Academic Press, 2nd ed., New York, 1968, p. 360, Chapter 43, Knowlton J. Caplan.

Storch, O.; Albrecht J.; Hejma J.; Kurfurst J.; Pojar K.; Urban J. "Industrial Separators for Gas Cleaning" Chem. Eng. Mono. **1979**, *6*, 92-113.

Strauss, W. *Industrial Gas Cleaning*, Pergamon Press Inc., Sydney, 1966.

Stairmand, C.J. "The design and performance of cyclone separator" *Trans. Inst. Chem. Eng.* **1951**, *29*, 356-383.

Swift, P. "The design and performance of cyclone separator" *Steam Heating Engr.* **1969**, *38*, 453.

Williamson, S.J. *Fundamentals of Air Pollution,* Addison-Wesley Publishing Co Inc., New York, 1973.

Wang, C.X.; Lin, Y.I. “Numerical simulation of three dimensional gas-particle flow in a spiral cyclone” *Appl. Math. Mech. (English Edition).* **2006,** *27(2),* 247-253.

Wang, J.J.; Wang, L.Z.; Liu, CW. “Effect of a stick on the gas turbulence structure in a cyclone separator” *Aerosol Sci. Tech.* **2005**, *39,* 713-721.

Woon-Fong, W.L.; Hung, C.H. “Investigation of pressure drop evolution of fibrous filter operating in aerodynamic slip regime under continuous loading of sub-micron aerosols” *Sep. Pur. Technol.* **2008**, *63,* 691-700.

Wolfgang, H.K.; Vincent, C. *Air Pollution Engineerng,* McGraw-Hill Publication Co., New York, 1980.

Wu, C.: Tekasakul, P.; Namiki, H.: Otani, Y. “Collection performance of cyclone with unwoven fabrics attached to the inner wall of outlet tube” *Aerosol Air Qual. Res.* **2000.**

Zhao, B.; Shen, H.; Kang, Y. “Development of a symmetrical spiral inlet to improve cyclone separator performance” *Powder Technol.* **2004**, *145,* 47-50.

VITAE

Name Mr. Mason Sangkhamanee

Student ID 4822141

Educational Attainment

Degree	Name of Institution	Year of Graduation
B.Sc. (Chemistry)	Prince of Songkla University	1997

Scholarship Awards during Enrolment

The scholarship from Higher Education Development Project: the Center of Excellence for Innovation in Chemistry (PERCH-CIC), funded by The Royal Thai Government (PERCH-CIC).